

## ORIGINAL ARTICLE



WILEY

# Fabrication and characterization of Ag- and Ga-doped mesoporous glass-coated scaffolds based on natural marine sponges with improved mechanical properties

Francesca E. Ciraldo<sup>1</sup> | Marcela Arango-Ospina<sup>1</sup> | Wolfgang H. Goldmann<sup>2</sup> | Ana M. Beltrán<sup>3</sup> | Rainer Detsch<sup>1</sup> | Alina Gruenewald<sup>1</sup> | J. A. Roether<sup>4</sup> | Aldo R. Boccaccini<sup>1</sup>

<sup>1</sup>Institute of Biomaterials, Department of Materials Science and Engineering, University of Erlangen-Nuremberg, Erlangen, Germany

<sup>2</sup>Institute of Biophysics, Department of Physics, University of Erlangen-Nuremberg, Erlangen, Germany

<sup>3</sup>Department of Materials Science and Engineering, Escuela Politécnica Superior, Universidad de Sevilla, Seville, Spain

<sup>4</sup>Institute of Polymer Materials, Department of Materials Science and Engineering, University of Erlangen-Nuremberg, Erlangen, Germany

## Correspondence

A. R. Boccaccini, Institute of Biomaterials, Department of Materials Science and Engineering, University of Erlangen-Nuremberg, Cauerstraße 6, 91058 Erlangen, Germany.  
Email: aldo.boccaccini@ww.uni-erlangen.de

## Funding information

European Commission, Grant/Award Number: Horizon 2020; CoACH ETN project, Grant/Award Number: 642557; TEM facilities of CITIUS-US, Grant/Award Number: Grant P2017/837-University of Seville; German Science Foundation, Grant/Award Number: DFG, Go598

## Abstract

Natural marine sponges were used as sacrificial template for the fabrication of bioactive glass-based scaffolds. After sintering at 1050°C, the resulting samples were additionally coated with a silicate solution containing biologically active ions (Ag and Ga), well-known for their antibacterial properties. The produced scaffolds were characterized by superior mechanical properties (maximum compressive strength of 4 MPa) and total porosity of ~80% in comparison to standard scaffolds made by using PU foam templates. Direct cell culture tests performed on the uncoated and coated samples showed positive results in terms of adhesion, proliferation, and differentiation of MC3T3-E1 cells. Moreover, vascular endothelial growth factor (VEGF) secretion from cells in contact with scaffold dissolution products was measured after 7 and 10 days of incubation, showing promising angiogenic results for bone tissue engineering applications. The antibacterial potential of the produced samples was assessed by performing agar diffusion tests against both Gram-positive and Gram-negative bacteria.

## KEYWORDS

antibacterial, bioactive glass, bone tissue engineering, ion delivery, scaffolds, VEGF

## 1 | INTRODUCTION

Although bone has the capability to regenerate itself without forming a scar, it cannot heal in case of so-called critical size defects. Autografts are nowadays still considered “the gold standard” for bone grafting due to their biocompatibility.<sup>1</sup>

Drawbacks of this approach include infection risk at the donor site, pain for the patient, prolonged hospitalization and rehabilitation

periods as well as the extra operating time required for treating both the implant and donor sites.<sup>2-5</sup> A valid alternative is provided by tissue engineering (TE), which involves the support of damaged tissue regeneration by the use of engineered biomaterials called scaffolds. One of the main challenges of TE is the design of porous 3-D scaffolds to induce tissue regeneration.<sup>6</sup> In the case of bone TE, bioactive materials able to promote bone regeneration have been in the focus of significant research efforts in the last 20+ years.<sup>6</sup>

This is an open access article under the terms of the Creative Commons Attribution-NonCommercial-NoDerivs License, which permits use and distribution in any medium, provided the original work is properly cited, the use is non-commercial and no modifications or adaptations are made.

© 2020 The Authors. *Journal of Biomedical Materials Research Part A* published by Wiley Periodicals LLC.

The most studied and used silicate biomaterial for bone defect filling is 45S5 bioactive glass (BG) (also known as Bioglass), which was developed in 1971 by Hench et al.<sup>7</sup> Bioglass is a silicate glass with a nominal composition (in wt%) of 45% SiO<sub>2</sub>, 24.5% CaO, 24.5% Na<sub>2</sub>O, 6% P<sub>2</sub>O<sub>5</sub>, which is able to bond to both soft and hard tissue once in contact with biological fluids.<sup>8,9</sup> In several studies, it was demonstrated that dissolution products released from the bioactive glass surface enhance, on the one side, the formation of hydroxyl-carbonate-apatite (HCA) similar to the mineral phase of bone and, on the other side, osteogenesis and angiogenesis.<sup>10–14</sup> Bioactive glasses are used in bulk or particulate form in non-load bearing sites for dental and orthopedic applications.<sup>10,15</sup> On the other hand, porous 3-D BG scaffolds are not used in clinical applications yet. The main challenge is to fabricate 3-D scaffolds that combine high porosity and adequate mechanical strength and stability similar to natural bone. The first 3-D Bioglass-based scaffolds were developed by Chen et al in 2006,<sup>16</sup> who introduced the standard foam replica technique for the development of scaffolds with porosities >90%, using polyurethane (PU) foams as sacrificial templates. In subsequent studies, it was shown that those scaffolds do not possess suitable mechanical properties for use in load-bearing clinical applications.<sup>6,17</sup>

An alternative approach to fabricate BG-based scaffolds with increased mechanical strength is the reduction of the total porosity while maintaining pore interconnectivity and pore sizes adequate for new tissue ingrowth and vascularization. In the last years, porous BG-based scaffolds with higher mechanical properties have been produced by the foam replica method and a powder metallurgy approach,<sup>17,18</sup> or using alternative sacrificial templates, for example, marine natural sponges.<sup>6,19</sup> Samples fabricated with these techniques showed mechanical strength values comparable to those of trabecular bone (2–12 MPa).

Mesoporous bioactive glasses (MBG) are gaining significant attention in the field of bone repair and drug delivery applications.<sup>20–23</sup> As a result of their large surface area, tailored mesoporosity and ordered pore structure, MBG show faster apatite mineralization compared to non-mesoporous bioactive glasses and offer the possibility to be loaded with drugs or biomolecules, that is, introducing a local drug delivery function to the scaffold.<sup>20,24–27</sup> Different therapeutic ions have been incorporated into MBG during or after synthesis such as copper, lithium, boron, strontium, silver, cerium, and gallium because of their potential to promote the formation of new bone due to their stimulating effect on angiogenesis and osteogenesis.<sup>28–30</sup> In this work, sol-gel derived ordered mesoporous glasses doped with gallium or silver were employed to coat BG-based scaffolds applying the impregnation technique. Scaffolds were fabricated using 45S5 BG as the starting material and natural marine sponges as sacrificial templates. The scaffolds were coated using either Ag or Ga-doped mesoporous glass slurries. The ability of the produced glasses to form HCA on their surface was verified by immersing them in simulated body fluid.<sup>31</sup> The surface modifications of the scaffolds were evaluated using SEM and FTIR. The overall performance of the MBG-coated 3-D scaffolds in terms of biological activity and antibacterial effects was studied.

## 2 | MATERIALS AND METHODS

### 2.1 | Synthesis of ordered mesoporous glasses

Silver- and gallium-doped ordered mesoporous glasses (Ag-MBG and Ga-MBG) with a composition (in % mol.) of 78 SiO<sub>2</sub>-20 CaO-1.2 P<sub>2</sub>O<sub>5</sub>-0.8 AgO and 68.8 SiO<sub>2</sub>-20 CaO-1.2 P<sub>2</sub>O<sub>5</sub>-10 Ga<sub>2</sub>O<sub>3</sub>, respectively, were produced by an evaporation induced self-assembly process (EISA). Briefly, Pluronic F127 was dissolved in EtOH and HNO<sub>3</sub> overnight. Glass precursors were added under continuous stirring as follows: tetraethyl orthosilicate (TEOS), triethyl phosphate (TEP), calcium nitrate (Ca[NO<sub>3</sub>]<sub>2</sub>·4H<sub>2</sub>O) and silver (AgNO<sub>3</sub>) or gallium nitrate (Ga[NO<sub>3</sub>]<sub>3</sub>), with an interval between each addition of 3 hr. All reagents were used without further purification. Ga-MBG was characterized by means of scanning electron microscopy (SEM) (Zeiss, Oberkochen, Germany) in combination with energy dispersive spectroscopy (EDS) (Oxford Instruments, Abingdon, UK), which was used to qualitatively confirm the incorporation of gallium in the glass. The inner microstructure was investigated, using transmission electron microscopy (TEM) analysis operating at an accelerating voltage of 200 kV and small angle XRD (SAXRD). X-ray fluorescence (XRF) (Zetius, PANalytical) analysis was performed to confirm the gallium presence and to identify the chemical formulation of the glass. Fourier transformed infrared spectroscopy (FTIR) (4000–400 cm<sup>-1</sup>, 32 scans, Nicolet 6,700, Thermo Scientific, Waltham, MA) and SEM were used to analyze the samples after immersion in SBF. The used SBF solution was analyzed in terms of Ca, P, Si, Ag and Ga ion concentration, using inductively coupled plasma optical emission spectrometry. The Ag-MBG have been characterized in a previous work.<sup>32</sup>

### 2.2 | Fabrication of bioactive glass-based scaffolds

Melt-derived 45S5 bioactive glass powder (Schott Vitryxx, Mainz, Germany) of nominal mean particle size <2 μm was used to fabricate BG-based scaffolds and natural marine sponges "*Spongia Agaricina*" (SA) were used as sacrificial templates.<sup>6</sup> Marine sponges belong to the "Elephant Ears" family and were harvested in the Indo-Pacific Ocean (Pure Sponges, Solihull, UK). BG scaffolds were produced according to the foam replica technique described by Chen et al in 2006.<sup>16</sup> PVA with a ratio of 0.01 mol L<sup>-1</sup> was dissolved in deionized water at 80°C for and then BG powder was added using a concentration of 40 wt%. After cutting the foams in cylindrical shapes (Ø = 8 mm and h = 8 mm), they were dipped in the PVA/BG slurry for 10 min. Subsequently, the excess of slurry was manually removed and the coated foams were slowly dried at room temperature. The procedure was repeated a second time. Compressed air, as previously reported,<sup>6,32</sup> was applied this time to eliminate the excess of slurry. After drying, a heat treatment was necessary to burn out the natural marine sponges and to obtain the sintered structure. A temperature of 400°C for 1 hr was used to remove the sacrificial template and of 1,050°C for 1 hr to densify the structure. The resulting scaffolds were coated by Ga-MBG or Ag-MBG using the impregnation technique. Five hundred microliter

of the sol silicate solution was dropped onto the scaffold, the samples were then dried at room temperature for 24 hr and then they underwent a second heat treatment at 700°C for 3 hr (Figure 1). Where required, samples were labelled SA\_Ag-MBG and SA\_Ga-MBG to refer to Ag-MBG and Ga-MBG coated scaffolds, respectively.

### 2.2.1 | Characterization of coated scaffolds

The ability of the coated scaffolds to form HCA on their surfaces was verified by immersing them in simulated body fluid.<sup>31</sup> The surface modifications of the scaffolds were evaluated using SEM and FTIR. Also, the inner microstructure was investigated using transmission electron microscopy (TEM) operating at an acceleration voltage of 200 kV. The mechanical properties of the obtained samples were also evaluated before and after immersion in SBF up to 28 days. An ion release study was performed by means of ICP-OES device. The overall biological performance of the MBG-coated 3-D scaffolds in terms of cell biology activity and antibacterial effects was evaluated. Indirect and direct cell culture tests were performed to prove the biocompatibility of the samples against MC3T3-E1 mouse derived pre-osteoblasts. Agar diffusion tests were carried out using both Gram-positive (*S. carnosus*) and Gram-negative (*E. coli*) bacteria.

### 2.3 | Indirect cell culture

Indirect cell culture tests were carried out following the general guidance set by the International Standardization Organization (ISO 10993-5:2009). Samples were sterilized at 160°C for 2 hr and placed in contact with cell culture medium for 24 hr in a culture incubator at 37°C and 5% CO<sub>2</sub>. The ratio mass/volume used was 0.1 g ml<sup>-1</sup> as recommended by the ISO standard. At the end of the incubation time,

the supernatant was collected and diluted to obtain the following concentrations: 100, 50, and 25%, which were used for the test. MC3T3-E1 osteoblast like-cells were placed in contact with the conditioned media and incubated for 48 hr at 37°C and 5% CO<sub>2</sub>. The influence of the different glasses on the cell viability was assessed using a WST-8 assay (Sigma-Aldrich, Germany). At the end of the cultivation period the activity of MC3T3-E1 cells was measured through the conversion of tetrazolium (WST-8) to formazan by intracellular enzymes. A solution containing 1 vol% WST reagent and 99 vol% α-MEM was prepared. The cell culture medium was removed, cells were washed with PBS and 300 μl of WST solution was added to each well. The cells were then incubated for 3 hr at 37°C and 5% CO<sub>2</sub>. At the end of the incubation time, 100 μl of the solution was taken from the samples and transferred into a 96-well plate. The absorbance was measured at 450 nm (PHOmo, Anthos, Germany). Results are presented as mean value and standard deviation of six replica of each sample type. All the samples were normalized to 0 wt/vol. Six percentage DMSO was used as the negative control. One-way analysis of variance (ANOVA) was used to evaluate the differences in analysis parameters between the different dilution concentrations and the different glass types. The level of significance was defined at  $p < .05$  (Origin 8.1, Origin Lab Corporations, USA). The significance levels were set as  $p < .05 = *$ ,  $p < .01 = **$  and  $p < .001 = ***$ . The Bonferroni test was used for comparison of the mean values.

### 2.4 | Direct cell test

Uncoated and coated scaffolds were tested using osteoblast-like cells. Both the cell viability and proliferation capability were investigated. Direct cell culture tests were performed to investigate cell behavior, once in contact with BG scaffolds. From the literature, it is well known that a pre-conditioning treatment is necessary to avoid a rapid

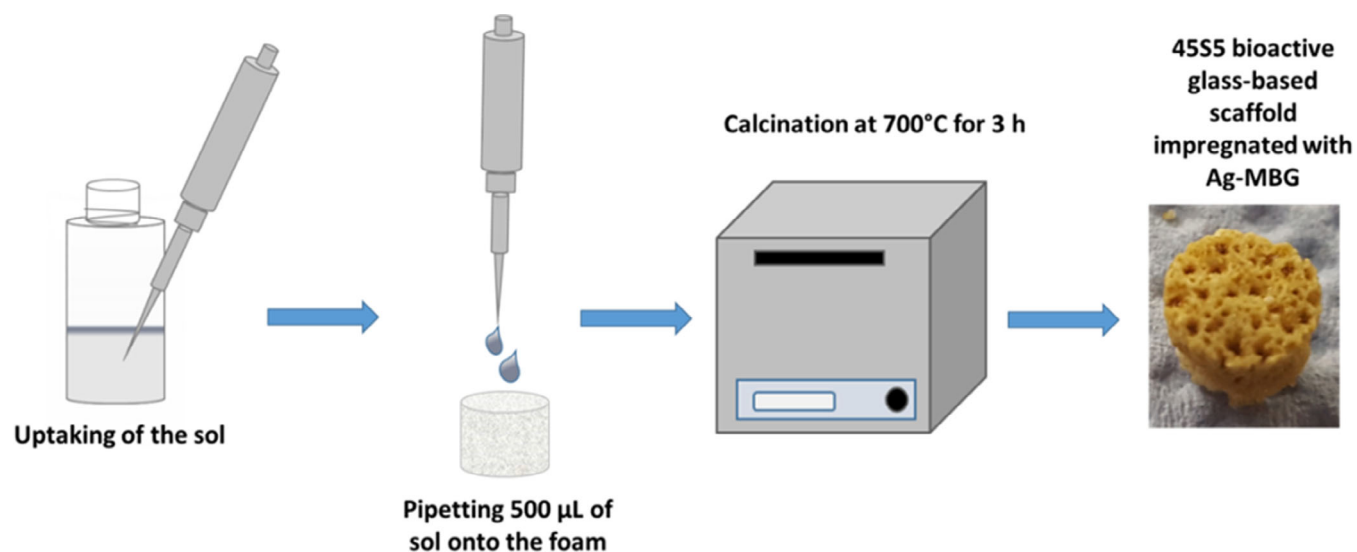


**FIGURE 1** Schematic diagram showing the fabrication of ordered mesoporous coated-BG based scaffolds (Ag-MBG coated scaffold as example)

increase of pH, which will make in vitro cell culture tests difficult or even impossible.<sup>31</sup> In the present work, every scaffold was sterilized by means of dry heat at 160°C for 3.5 hr and pre-conditioned in 1 ml of cell culture medium in an incubator at 37°C and 5% CO<sub>2</sub> until the pH was lower than eight. The medium was changed every day to better simulate the physiological conditions, where a continuous wash-out of the ions takes place.

### 2.4.1 | Cell seeding

MC3T3-E1 cells were chosen to perform the experiments. This cell line can differentiate into osteoblasts and thus the cells are relevant for the present study as they promote formation of calcified bone tissue. Mineral deposits have been identified as hydroxyapatite. They were cultured in high glucose alpha-MEM supplemented with 10 vol% of fetal bovine serum (FBS) and 1 vol% of penicillin-streptomycin (PenStrep) and incubated at 37°C in a humidified atmosphere (95%) containing 5% CO<sub>2</sub>. Trypsinization was used to collect cells once they had reached confluency of between 80 and 100%. Trypan blue exclusion method was used to count cells. A concentrated cell suspension in a drop-wise manner was chosen to seed cells directly onto the scaffolds. A droplet of 50 µl containing 80,000 cells was used. After this procedure, scaffolds were incubated at 37°C, in 5% CO<sub>2</sub> for 45 min. Each well was then flooded with medium and cultured for 24 hr, 3, 7, and 10 days. Cell viability was measured by means of WST-8 metabolism and lactate dehydrogenase (LDH) activity. VEGF release was measured after 7 and 10 days of incubation. Cell morphology was observed by SEM analysis.

### 2.4.2 | VEGF production

Production of Vascular Endothelial Growth Factor (VEGF), known to be a fundamental biomolecule for the regulation of angiogenesis, was quantitatively measured using an ELISA (Enzyme-linked Immunosorbent Assay) kit (RayBio Mouse VEGF-A ELISA, Ray Biotech, Ins. Nocrass, GA). This assay consists of a well plate coated with a specific antibody for mouse VEGF. Aliquots of the culture medium from the direct test were taken after 7 and 10 days and transferred to the ELISA well plate. After 2.5 hr of incubation, the wells were washed with the provided wash buffer and then incubated with the following reagents: a biotinylated antibody for 1 hr, a streptavidin solution for 45 min, and a one-step substrate reagent for 30 min and finally a stop solution. Between incubation steps, the samples were washed using the provided buffer. Once the stop solution was added, the absorbance at 450 nm was read immediately. The intensity of the colored solution is directly proportional to the concentration of VEGF secreted by the MC3T3-E1 cells in the presence of the samples. In addition a standard curve was created according to the manufacturer's protocol to determine the unknown amount of VEGF in the samples.

### 2.4.3 | LDH activity

Lactate dehydrogenase (LDH) is an enzyme, which can be found inside cells and can be used to measure both the number of cells or their membrane integrity. Cell numbers can be measured by total cytoplasmic lactate dehydrogenase; the membrane integrity depends on the amount of cytoplasmic LDH released in the medium. The main reaction characteristic of the assay is the reduction of NAD by LDH, which leads to a reduced NADH. A stoichiometric reaction is used to convert the reduced NADH in a tetrazolium dye, a colored compound that can be detected spectrometrically.

The amount of LDH is proportional to the cell number. Cells, which were attached to the scaffolds, were lysed after 1, 3, 7, and 10 days of incubation using a lysis buffer (0.1 wt% Triton X, 20 mM TRIS, 1 mM MgCl<sub>2</sub> and 0.1 mM ZnCl<sub>2</sub>) and centrifuged. A mastermix was prepared according to the manufacturer's protocol (TOX-7, Sigma-Aldrich). Twenty microliter of dye solution was mixed with 20 µl of cofactor preparation and 20 µl of substrate solution. Afterwards, 140 µl of the supernatant was mixed with 60 µl of mastermix and incubated at room temperature for 30 min. During this incubation time, NADH is used to transform a tetrazolium salt to formazan. The reaction was then stopped by adding 300 µl of HCl 1 M. UV-VIS (Specord 40, Analytic Jena) spectroscopy was used to measure the absorbance at 490 and 690 nm.

### 2.4.4 | Osteocalcin production

Osteocalcin, also known as bone gamma-carboxyglutamic acid-containing protein (BGLAP), is a non-collagenous protein hormone, which can be found in bone and dentin. Osteocalcin is secreted by osteoblasts, and it is involved in bone mineralization. Osteocalcin was quantitatively measured using an ELISA kit (Abbexa, Mouse Osteocalcin (BGLAP) ELISA Kit, Cambridge, UK). Absorbance measurements were used to determine the amount of osteocalcin present in the samples. The absorbance of both, the unknown sample and the standard solutions of a known OC concentration, were measured. By means of indirect calculation, the unknown OC concentration was obtained.

## 2.5 | Antibacterial test

Antibacterial tests were carried out to verify the efficacy of silver and gallium ions against both Gram (+) and Gram (-) bacteria. Two strains were selected to perform antibacterial tests: *Staphylococcus epidermidis* as Gram (+) and *Escherichia coli* as Gram (-).

Antibacterial agar diffusion tests were also performed using *Staphylococcus Carnosus* (Gram (+)). A solution containing bacteria was prepared by suspension in lysogeny broth (LB) medium and the optical density (O.D.) was adjusted (600 nm, Biphotometer Plus, Eppendorf AG, Hamburg, Germany) to obtain a value of 0.015, following a protocol established in our laboratory. Twenty microliter of the prepared



suspension was pipetted and homogeneously spread onto a petri dish (10 cm diameter), previously covered with a layer of LB Agar. The scaffolds, uncoated and coated, were positioned on the agar and the culture was placed in an incubator at a temperature of 37°C and a high relative humidity (80%). After 24 hr the formation of an inhibition zone around the samples was assessed.

### 3 | RESULTS

#### 3.1 | Characterization of Ga-MBG

XRD analysis was performed on the synthesized gallium-doped mesoporous glass. No diffraction peaks were detected, indicating that the glass is amorphous. No crystalline phase developed during the heat treatment, since a broad peak in the range  $2\theta = 20\text{--}35^\circ$  is visible in the XRD pattern, shown in Figure 2(a). Figure 2(b,c) show a characteristic TEM micrograph and a typical SAXRD pattern of the synthesized Ga-MBG, respectively. Different particles were analyzed, leading to the conclusion that Ga-MBG is characterized by an ordered 2-D hexagonal structure. This was also confirmed by SAXRD analysis. On the

SAXRD pattern shown in Figure 2(c), it is possible to observe two peaks at  $2\theta$  1–1.4° and around 2°, typical for mesoporous bioactive glasses. Results are in accordance with those found by Lopez-Noriega et al.<sup>33</sup> Lopez-Noriega et al suggest that the presence of this pattern is typical of an hexagonal arrangement with 1-D pore channel structure.

XRF analysis was performed to confirm the incorporation and maintenance of the elements in the MBG matrix after calcination at 700°C. Other trace elements (ppm) were identified, potentially as result of minor contamination occurred during the synthesis of the glass. The chemical composition (wt.%) resulting from the XRF analysis was: 10.9% SiO<sub>2</sub>, 19% CaO, 1% P<sub>2</sub>O<sub>5</sub> and 10% Ga<sub>2</sub>O<sub>3</sub>.

The ability of the MBG to form a HCA layer on its surface was assessed by immersing the powder in SBF for up to 7 days (Figure 3). The formation of a layer of HCA was observed using SEM, after 1 day of soaking in SBF. After 3 and 7 days of immersion, HCA covers the surface of the glass homogeneously. The presence of HCA was also confirmed by FTIR and XRD. Results are reported in Figures 4 and 5. Typical characteristic bands at 560 and 604 cm<sup>-1</sup> (P–O bending), and at 874 cm<sup>-1</sup> (CO<sub>3</sub><sup>2-</sup>) can be detected after 3 days of immersion in SBF. The P–O bending bands confirm the

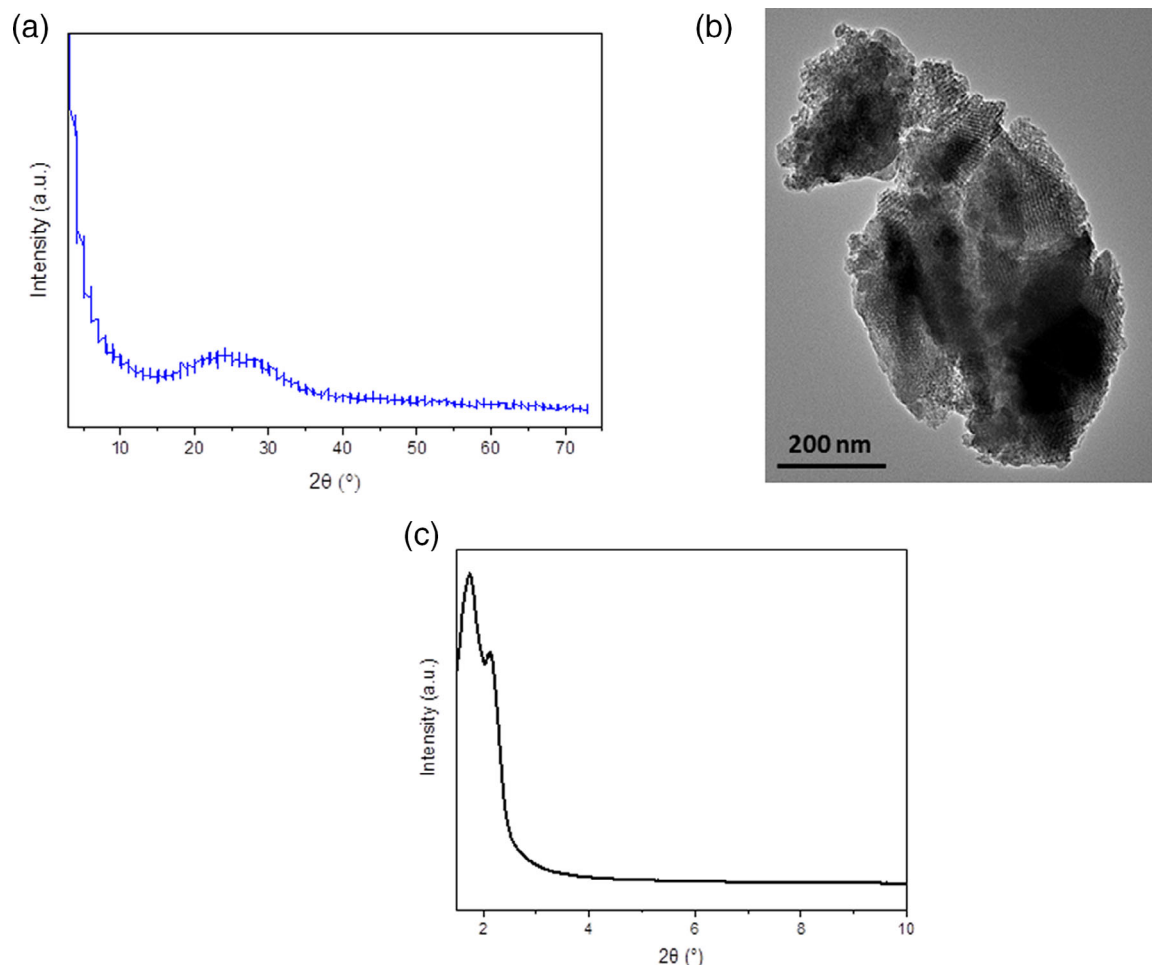


**FIGURE 2** XRD pattern of Ga-MBG (a), TEM micrograph showing the ordered mesoporosity of Ga-MBG (b) and SAXRD pattern of Ga-MBG (c)

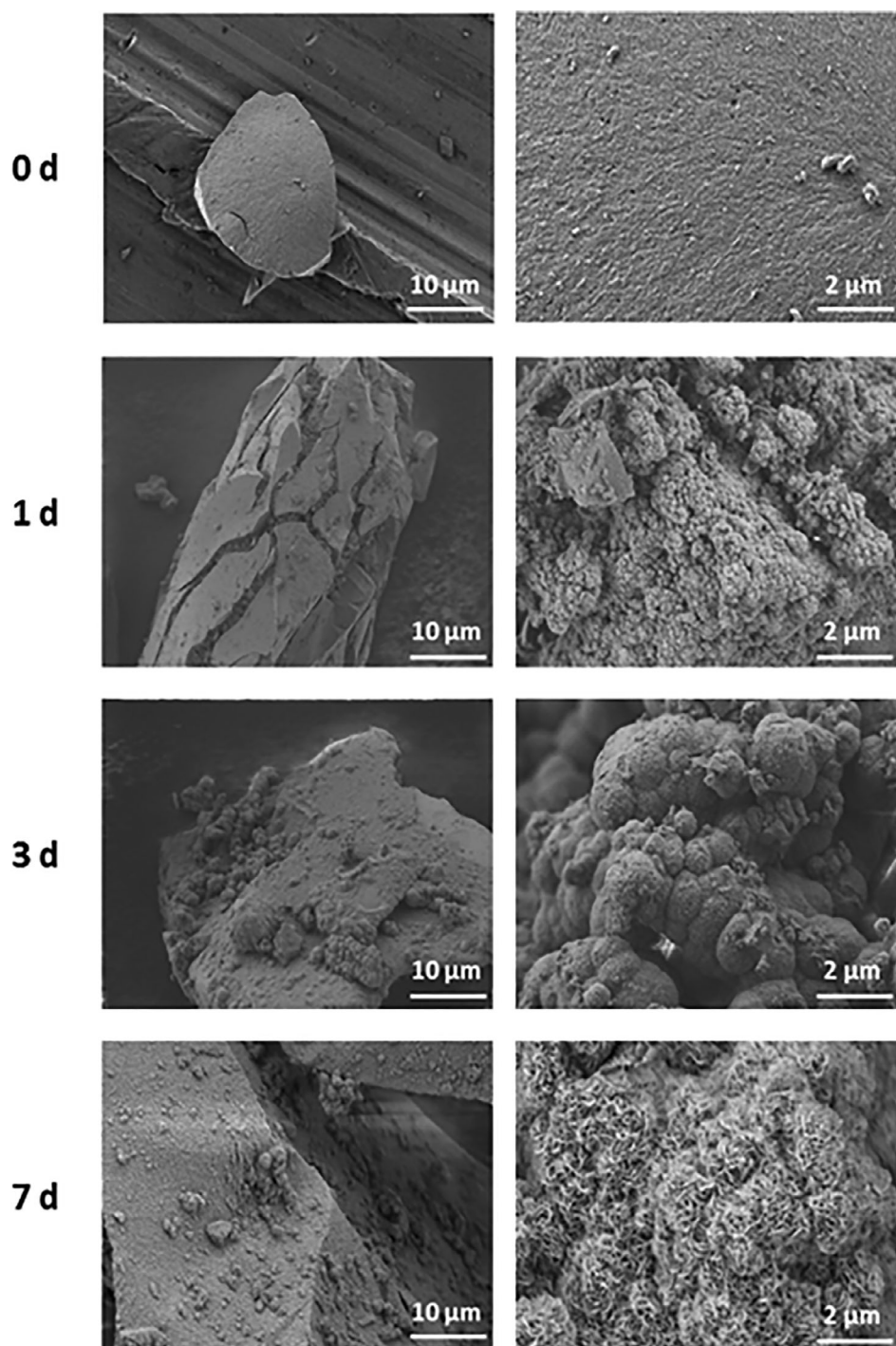


**FIGURE 3** SEM micrographs of Ga-MBG after 0, 1, 3, and 7 days of immersion in SBF. Already after 72 hr it is possible to observe the presence of HCA characterized by a typical cauliflower-like structure

presence of HCA on the surface of the samples.<sup>34</sup> FTIR results verified the XRD analyses of samples soaked in SBF for up to 3 days. As shown in Figure 2(a), the as-produced sample spectra present a very broad peak for  $2\theta$  values between  $20$  and  $35^\circ$ . However, XRD spectra of the samples soaked in SBF (Figure 5) indicate two new peaks at  $2\theta$  around  $26$  and  $32^\circ$  in comparison with the XRD spectrum reported in Figure 2, which may correspond to the (002) and (112) planes of HCA (although a more detailed XRD study would be required to confirm this assumption).

The modification of SBF composition during bioactivity studies was used as an indirect method to investigate the process occurring on the glass surface. The unchanged SBF was analyzed using ICP-OES measurements. Results are reported in Figure 6. It is well-known that bioactive glasses start to exchange ions with the surrounding environment once in contact with water-based solutions.<sup>35</sup> Moreover, an initial increase in Ca, P, and Si ions followed by a decrease in P ions in the solution indicates the start of formation of a calcium-phosphate layer on the surface of the glass.<sup>31</sup>

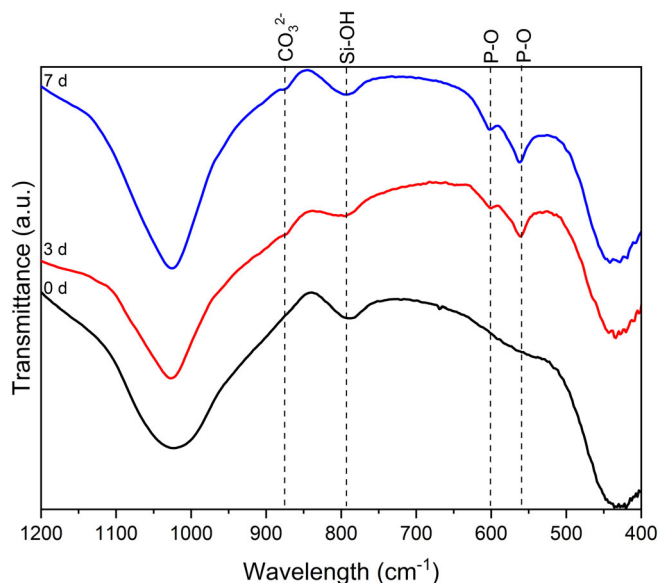


**FIGURE 4** Graph showing the Ga-MBG FTIR spectra before and after immersion in SBF. Spectra after 3 and 7 days are displayed

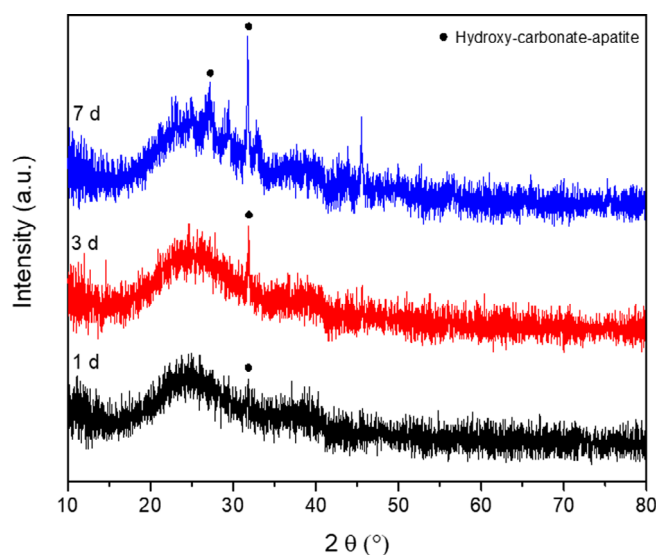


**FIGURE 5** XRD analysis results on Ga-MBG samples after immersion in SBF for 0, 3, and 7 days

In this study, the release of silicon from Ga-MBG after 3 days of immersion in SBF was around  $20 \text{ mg L}^{-1}$ . After 8 hr, the concentration of calcium reached  $50 \text{ mg L}^{-1}$ , and after 3 days  $80 \text{ mg L}^{-1}$  was released from the glass. Concerning the release of gallium, it is possible to observe that the maximum release of Ga ions occurs after 72 hr. The same evidence was found by Salinas et al.<sup>36</sup> The authors corroborate the hypothesis that  $\text{Ga}^{3+}$  can act as intermediate glass network or as network former, depending on the glass composition. The location of  $\text{Ga}^{3+}$  ions in the glass network can therefore either support or hinder the release of ions into the surrounding medium.<sup>36</sup> However, after 3 days of immersion in SBF, the release

of  $\text{Ga}^{3+}$  did not reach an equilibrium, suggesting that not all the ions had been released from the glass matrix.

## 3.2 | Characterization of MBGs-coated scaffolds

### 3.2.1 | Morphological characterization and bioactivity evaluation

The presence of a homogeneous coating on the 45S5 bioactive glass scaffolds was assessed by means of SEM (Figure 7). It can be observed that before the application of the MBGs coating, the surface of the BG-based scaffold appears rough and the individual glass particles can still be observed. After the coating with MBG, the surface appears smoother, suggesting the presence of a new layer. This hypothesis was confirmed by EDS analysis, which revealed the presence of Ag and Ga on the surface of the samples. Since Ag and Ga ions are not present in 45S5 BG used for making the scaffolds, the results confirm that the MBG coating was successfully applied.

Coated scaffolds were immersed in SBF for up to 3 days to verify that the double heat treatment they were subjected to did not affect their ability to form HCA in contact with physiological fluids. 45S5 BG-based scaffolds were used as reference. SEM micrographs shown in Figure 8 illustrate that after only 1 day of immersion in SBF, the surface of the samples (uncoated 45S5 BG scaffolds and Ag-MBG coated scaffolds) is homogeneously covered by a layer of HCA. A delay in the formation of HCA can be observed for the scaffolds coated with Ga-MBG. After 3 days of immersion in SBF, it was possible to detect the formation of a hydroxycarbonate apatite layer.

FTIR analysis confirmed the presence of a HCA layer on the samples. On the spectra reported in Figure 9 it is possible to observe the presence of two P–O bending peaks at around  $560$  and  $640 \text{ cm}^{-1}$  and a band at  $874 \text{ cm}^{-1}$ , which can be attributed to carbonate.<sup>34</sup> Moreover, a variation of three peaks corresponding to the stretching of Si–O–Si ( $800 \text{ cm}^{-1}$  and  $1,070 \text{ cm}^{-1}$ ) and silanol bonds (at  $960 \text{ cm}^{-1}$ ) was detected after immersion in SBF.<sup>37</sup>

### 3.2.2 | Mechanical properties and stability

The compressive strength of scaffolds was measured as a function of soaking time in SBF. The maximum compressive strength was determined measuring 10 samples for each time point (Figure 10). Before immersion in SBF, all samples showed similar compressive strengths reaching a value of  $4 \pm 1 \text{ MPa}$ . Similar results were obtained by Boccardi et al using a system with only Bioglass 45S5.<sup>17</sup> A typical stress-deformation curve is shown in Figure 10 for SA\_Ga-MBG. Similar results were obtained for SA\_45S5 and SA\_Ag-MBG. After 7 days of immersion in SBF, a reduction of more than 50% from the initial maximum compressive strength was determined. The final values were:  $1.8 \pm 0.2 \text{ MPa}$ ,  $1.2 \pm 0.2$  and  $0.6 \pm 0.3$  for SA\_45S5, SA\_Ag-MBG, and SA\_Ga-MBG, respectively. After immersion in SBF, a significant decrease of the

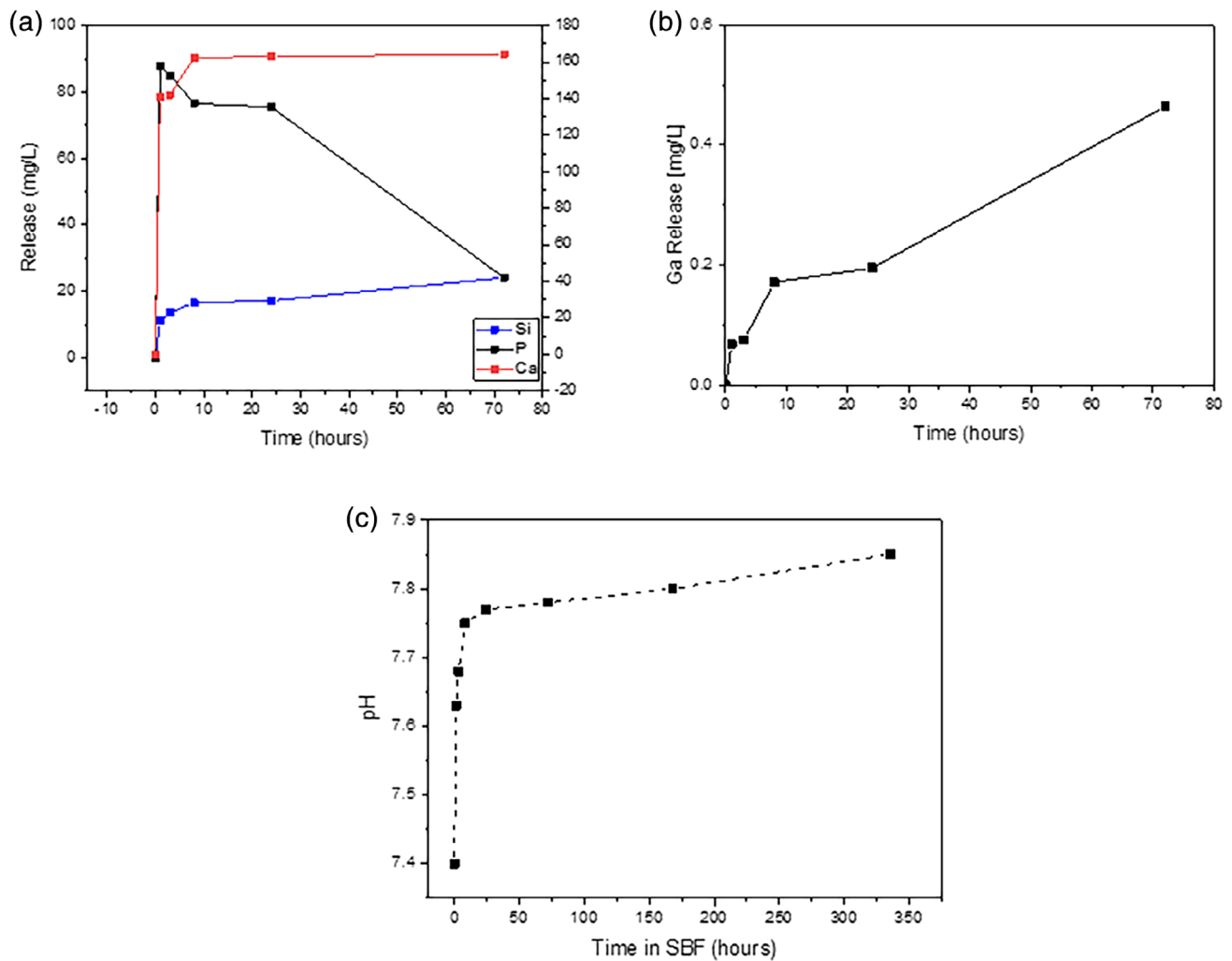


**FIGURE 6** Graphs showing the ion release in SBF as function of time. Si, Ca, and P (a) and Ga (b). The pH variation of the unchanged SBF is shown in (c)

weight and an increase of the total porosity were visible for both, SA\_Ag-MBG and SA\_Ga-MBG. Both kinds of scaffolds showed a loss of around 25% of their starting weight after 28 days of immersion in SBF. Concerning the porosity variation, as shown in Figure 11, SA\_Ag-MBG reached a porosity of 90% and SA\_Ga-MBG a porosity of around 85% after 28 days of SBF immersion. The main weight loss, together with the main compressive strength change and porosity variation, were observed after the first 7 days of immersion in SBF, probably due to the dissolution of the glass. A similar trend was observed for SA\_45S5 scaffolds in terms of porosity and weight variation. A smaller weight variation was observed for SA\_Ag-MBG and SA\_Ga-MBG scaffolds in comparison with SA\_45S5 suggesting that the presence of a coating may slow down the dissolution of the glass.

### 3.2.3 | Ion release and pH variation

The ion concentration in SBF and the pH variation up to 21 days of immersion are shown in Figure 12. From the ion release profiles it can

be observed that the release of Si, Ca, and P ions takes place immediately for both SA\_Ag-MBG and SA\_Ga-MBG samples. The ion release profiles for both types of scaffolds show a similar trend. The pH of the Ag-MBG coated scaffolds exhibited a faster pH increase, up to a maximum of 8.1 after 21 days of immersion in SBF. On the contrary, samples coated with Ga-MBG were characterized by a slower pH increase, which reached its equilibrium at pH 7.9 after 14 days of soaking in SBF. After 21 days of immersion in SBF, Si was present in concentration of 180 and 60 ppm, for SA\_Ga-MBG and SA\_Ag-MBG, respectively. Ca concentration increased up to 220 ppm at the end of the test, and P concentration decreased over time, suggesting the formation of a P-containing layer on the surface of the scaffolds during soaking in SBF. The therapeutic ions were also detected; the release profile of Ag did not increase linearly probably due to the precipitation of insoluble AgCl, on the surface, as already observed for Ag-MBG powders. The Ga ion release profile increases continuously, reaching around 20 ppm after 21 days of immersion in SBF. Also in this case, as already mentioned for the ICP test of the powder, the leaching of Ga seems to be slower in the first 24 hr of immersion. This result can



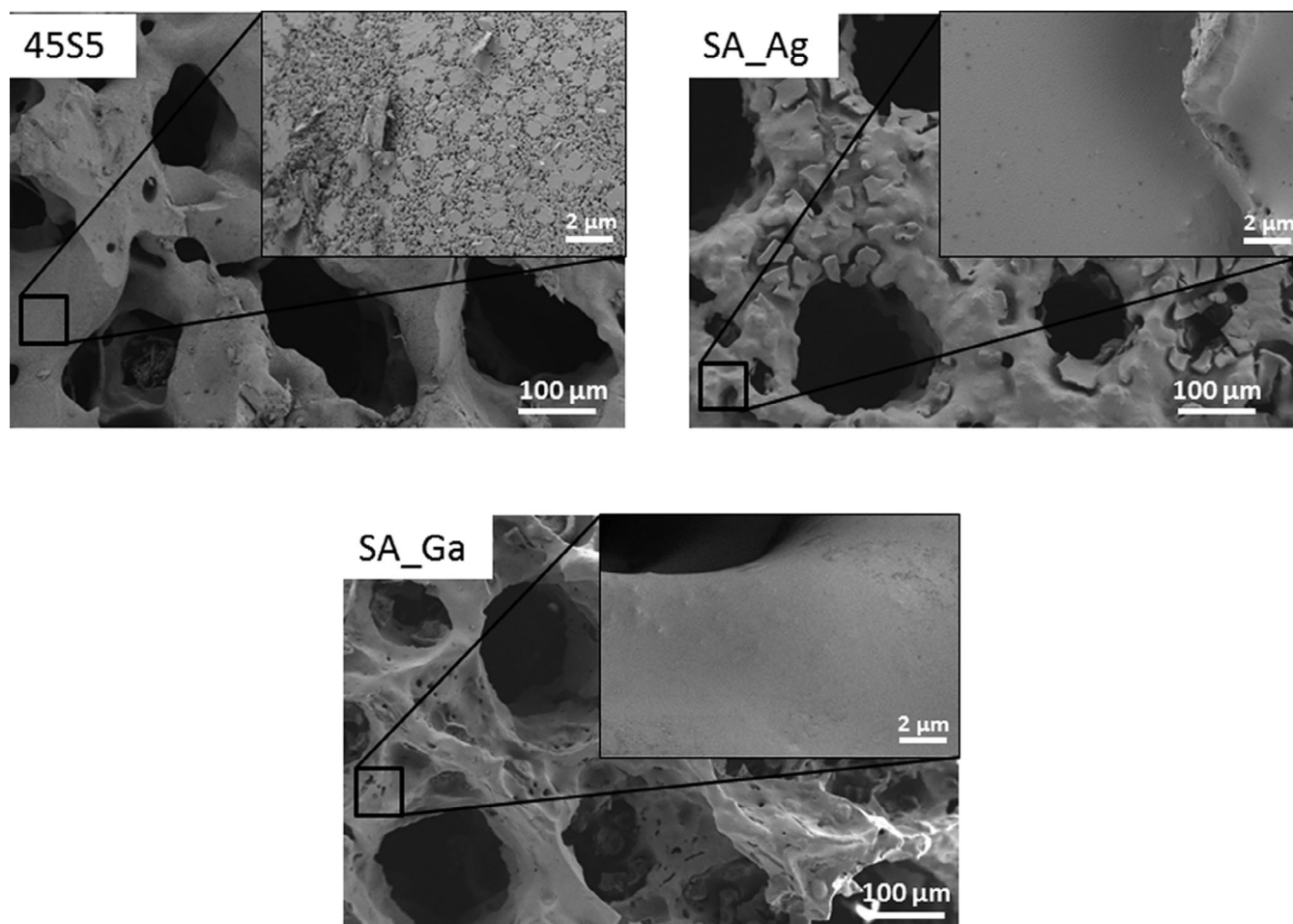


**FIGURE 7** SEM micrographs showing the morphology of bare (uncoated) 45S5 BG scaffold, and Ag (SA\_Ag), and Ga (SA\_Ga) MBG coated scaffolds

be attributed to the location of  $\text{Ga}^{3+}$  ions in the glass network, which might either favor or delay the ion release into the surrounding medium.

### 3.3 | Indirect cell culture test

The results about viability and morphology of MCT3-E1 cells tested for indirect cytotoxicity are displayed in Figures 13 and 14. Figure 13 shows the viability of MC3T3-E1 cells when placed in contact with different concentrations of BG scaffold powder. Cells cultured only with cell culture medium were used as reference and were normalized to 100%. Live staining with calcein acetoxymethyl-ester (Calcein AM, Invitrogen, USA) was carried out after 48 hr of cultivation to prove cell viability. The nuclei were visualized by blue nucleic acid stain, DAPI (4',6-diamidino-2-phenylindole, dilactate, Invitrogen, USA), known for preferentially binding to A (Adenine) and T (Thymine) regions of DNA. The images of calcein-DAPI-stained-cells were taken using a fluorescence microscope (Axio Scope A.1, Carl Zeiss Micro-imaging GmbH, Germany).

From Figure 14, it is possible to observe that the pre-osteoblasts exhibit their phenotypical morphology and that they adhere to the surface of the well plate. Although Figure 14 shows a higher cell density for Ag- and Ga-coated BG based scaffolds in comparison to the reference (BG uncoated scaffold), the morphology and the spreading of the pre-osteoblast cells was similar for all tested samples.

### 3.4 | Direct cell culture test

#### 3.4.1 | Cell viability

MC3T3-E1 cells were also directly seeded onto uncoated and coated BG-based scaffolds in 24-well culture plates and cultured for up to 10 days. At the end on each time point, the viability of the cells was assessed through WST measurements and the morphology was analyzed by SEM.

After 24 hr of incubation at 37°C and 5%  $\text{CO}_2$ , cell adhesion to uncoated and coated scaffolds was verified by SEM (Figure 15).



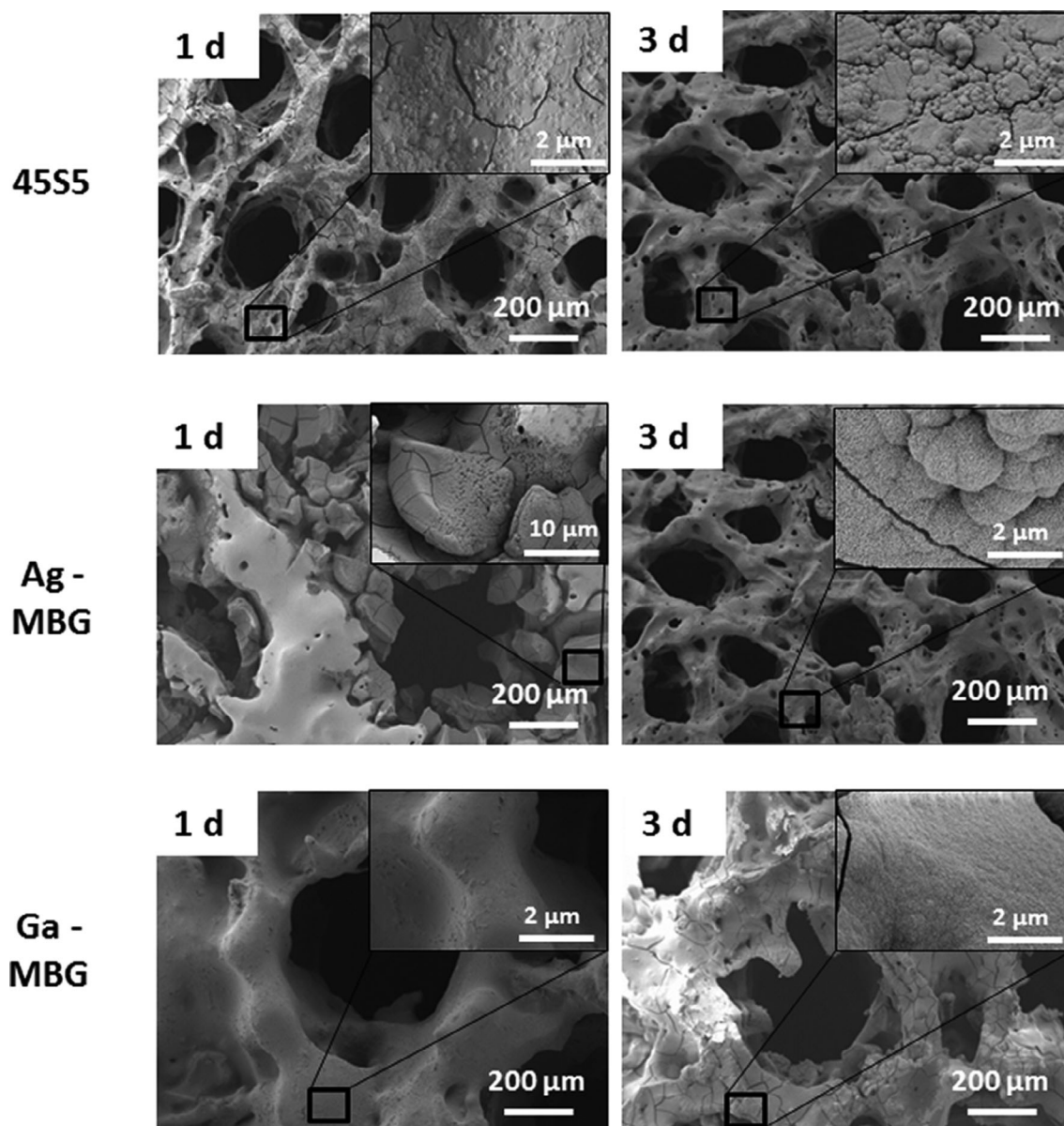


**FIGURE 8** SEM micrographs of uncoated and coated scaffolds after 1 and 3 days of soaking in SBF. The presence of HCA was detected after 72 hr of immersion for uncoated 45S5 BG, Ag-MBG, and Ga-MBG coated scaffolds

Already after 24 hr, attachment of cells to the different substrates was detected. However, it was possible to observe the presence of more cells on Ga-MBG coated scaffolds. These results were confirmed by WST-8 measurement (Figure 16). The cell viability on coated scaffolds was comparable to that of the control, suggesting that the presence of silver and gallium did not affect the biocompatibility of the samples.

As previously discussed, a pre-conditioning treatment of the scaffolds prior to cell culture was performed. This step is necessary to be able to carry out cell culture tests,<sup>35</sup> but it might remove therapeutic ions present in the coating. To confirm that the ions were still present after the pre-conditioning, EDS was performed on pre-treated samples after 24 hr of cell culture. As

reported in Figure 17 for a Ga-MBG sample, EDS indicates that Ga was still present on the coating surface. Moreover, these findings confirm the results obtained by ICP-OES analysis in that after 3 days of immersion in SBF, gallium was still being released to the medium.

### 3.4.2 | VEGF production

The VEGF release from MC3T3-E1 cells cultured in contact with 45S5 BG scaffolds, Ag- and Ga-MBG-coated scaffold is shown in Figure 18. The expression of VEGF was found to be highest (~1,605 pg/ml after 10 days) when cells were placed in contact with

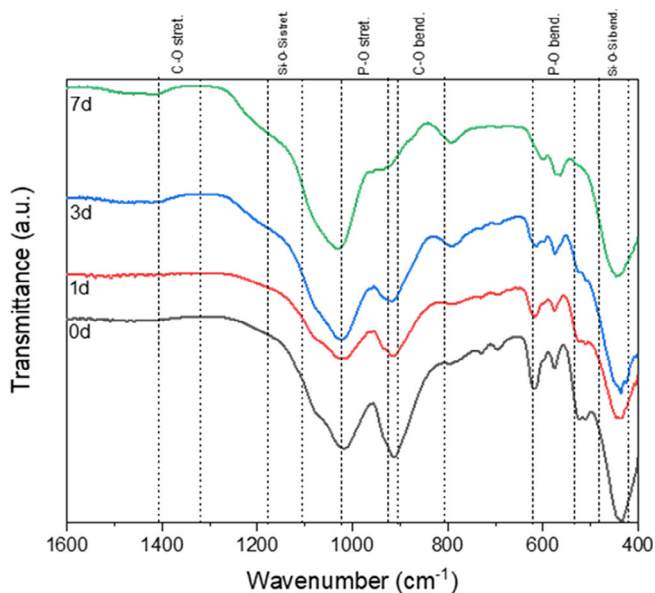


**FIGURE 9** FTIR spectra of Ag-MBG (a) and Ga-MBG (b) coated scaffolds before and after immersion in SBF at different time points; relevant bands are indicated in the spectra and discussed in the text

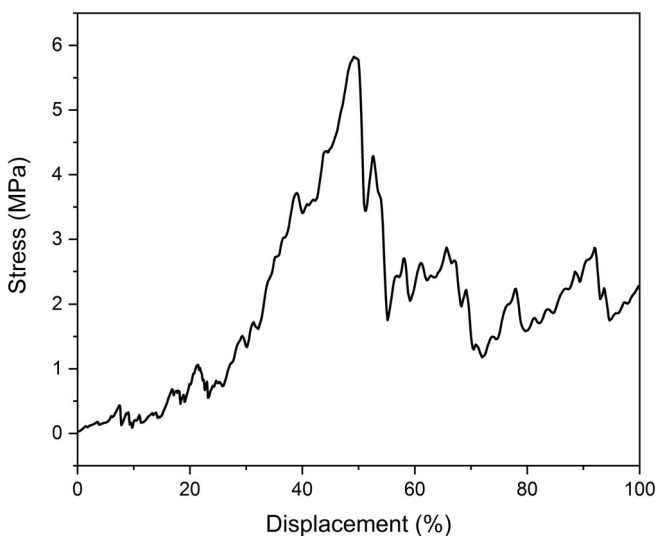


**FIGURE 10** Typical stress-displacement curve in compression for SA\_GA-MBG scaffold

Ga-MBG-coated scaffolds compared to uncoated 45S5 BG scaffolds. Ag-MBG scaffolds also exhibited significantly higher expression of VEGF when compared to 45S5 BG scaffolds.

### 3.4.3 | LDH activity

Figure 19 shows the results of LDH activity for different samples, measured after 7 and 10 days of incubation. From the graph, it is visible that a higher number of cells was detected on the Ga-MBG coated scaffolds in comparison to the uncoated and Ag-MBG coated

scaffolds, considering the linear correlation between LDH activity and the number of cells.

This result confirms the outcome of WST-8 measurements and SEM analysis. Moreover, no significant difference was observed between 7 and 10 days of incubation, suggesting that cells stopped proliferating and started the differentiation process.

The VEGF values were normalized with respect to the LDH ones to prove that VEGF secretion does not depend on the higher number of cells present on the scaffolds, but on the presence of the different therapeutic ions incorporated in the MBG coating (Ag or Ga). Results are shown in Figure 20. From the graph, it can be observed that after 7 days of culture, no significant differences exist between the uncoated 45S5 BG scaffolds and Ag-MBG and Ga-MBG coated scaffolds. However, after 10 days of incubation, VEGF expression values seem to be higher for the uncoated 45S5 BG and Ag-MBG coated scaffolds in comparison to the Ga-MBG-coated scaffolds. We hypothesize that Ag ions, released from the scaffolds surface, stimulate MC3T3-E1 cells to secrete higher amounts of VEGF compared to Ga-MBG-coated scaffolds.

### 3.4.4 | Osteocalcin production

Mineralized bone matrix and ECM components such as calcium phosphate and osteocalcin, produced by mature osteoblasts, are generally used as markers for assessing osteoblast differentiation at the later stage.<sup>38</sup> Moreover osteocalcin is deposited on the matrix but a small fraction can be released.<sup>39</sup> In this study, osteocalcin release into the medium was measured and is reported in Figure 21. After 1 week, osteocalcin production of 0.4 ng/ml was observed across all experimental groups. After 2 weeks, production of osteocalcin slightly increased for all tested samples. For both time points, no significant difference was observed between samples indicating that the MBG coated scaffolds supported the late stage of osteoblast differentiation.

### 3.5 | Antibacterial test

*Staphylococcus carnosus* (Gram (+)) and *Escherichia coli* (Gram (-)) bacteria were used to perform antibacterial agar diffusion tests, following a procedure previously published.<sup>32</sup> An inhibition zone, where bacteria did not grow around the coated scaffolds, was visible in both cases (see Figure 22, for Ag-MBG coated scaffolds). Tests were also carried out for samples after up to 3 days of immersion in SBF to verify their antibacterial properties. Even after 72 hr of soaking in SBF, it was possible to observe the presence of an inhibition zone, suggesting that silver was still present and could be still released from the coated scaffolds.

*Staphylococcus epidermidis* (Gram (+)) and *Escherichia coli* (Gram (-)) bacteria were selected as strains for further testing. Results are reported in Figure 23. Also, in this case after 24 hr of incubation, it was possible to observe an inhibition halo around the sample, where

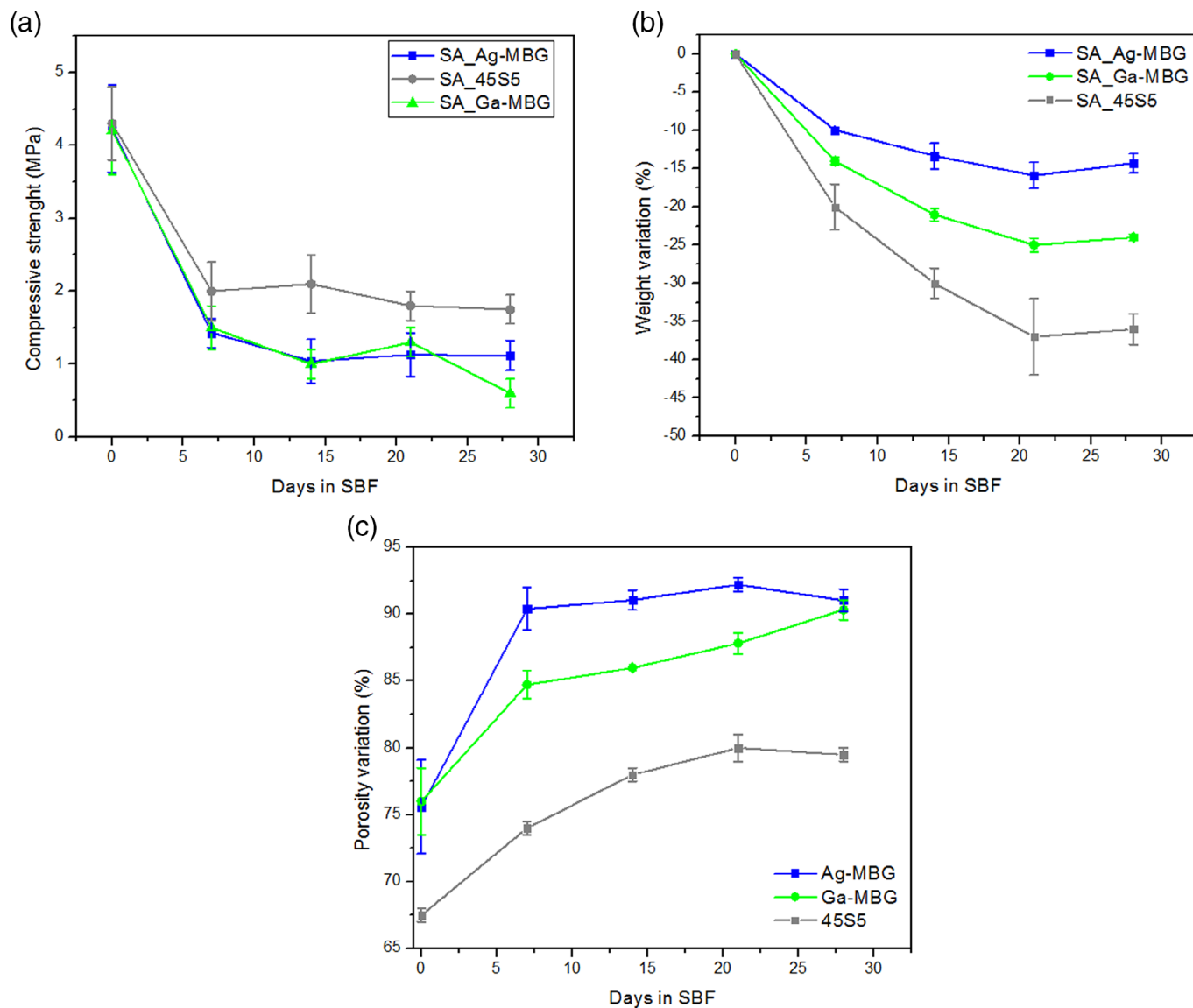


**FIGURE 11** Compressive strength, weight and porosity variation of coated 45S5 BG scaffolds after different immersion times in SBF for up to 28 days

no bacteria are present. It is also apparent that around the reference (uncoated 45S5 BG scaffold), an inhibition zone is visible, probably due to the increase of pH that takes place once the BG based samples get in contact with water-based solutions. However, the inhibition zone was small and difficult to measure. This can probably be related to the fact that the surface of the scaffolds is not regular, and they do not adhere completely to the agar surface.

## 4 | DISCUSSION

It is well-known that bone defects above a critical size cannot self-heal. They need osteo-inductive and osteo-conductive support to promote and support the regeneration of the new tissue.<sup>38</sup> Bioactive ceramics have been studied for many years and are considered

promising candidates in bone tissue engineering applications.<sup>10</sup> In particular, bioactive glasses have been used in bone replacement and tissue engineering applications due to their ability to bond to host tissue and to release ions that promote bone growth.<sup>9</sup> In this work, BG based scaffolds were fabricated by the foam replica method from 45S5 BG using natural marine sponges as sacrificial templates. The scaffolds were then impregnated with a silicate sol solution to obtain ion doped MBG coatings (Ag-MBG and Ga-MBG). A heat treatment followed the coating procedure to remove the structure directing agent and nitrates. Based on previous studies, one single impregnation was used for the coating of BG scaffolds.<sup>40</sup> In fact, Boccardi found that the increasing number of impregnation cycles led to an overflow of sol-gel glass.<sup>40</sup> Uncoated and coated scaffolds were characterized in terms of morphology, mechanical properties, and bioactivity once in contact with biological fluids.

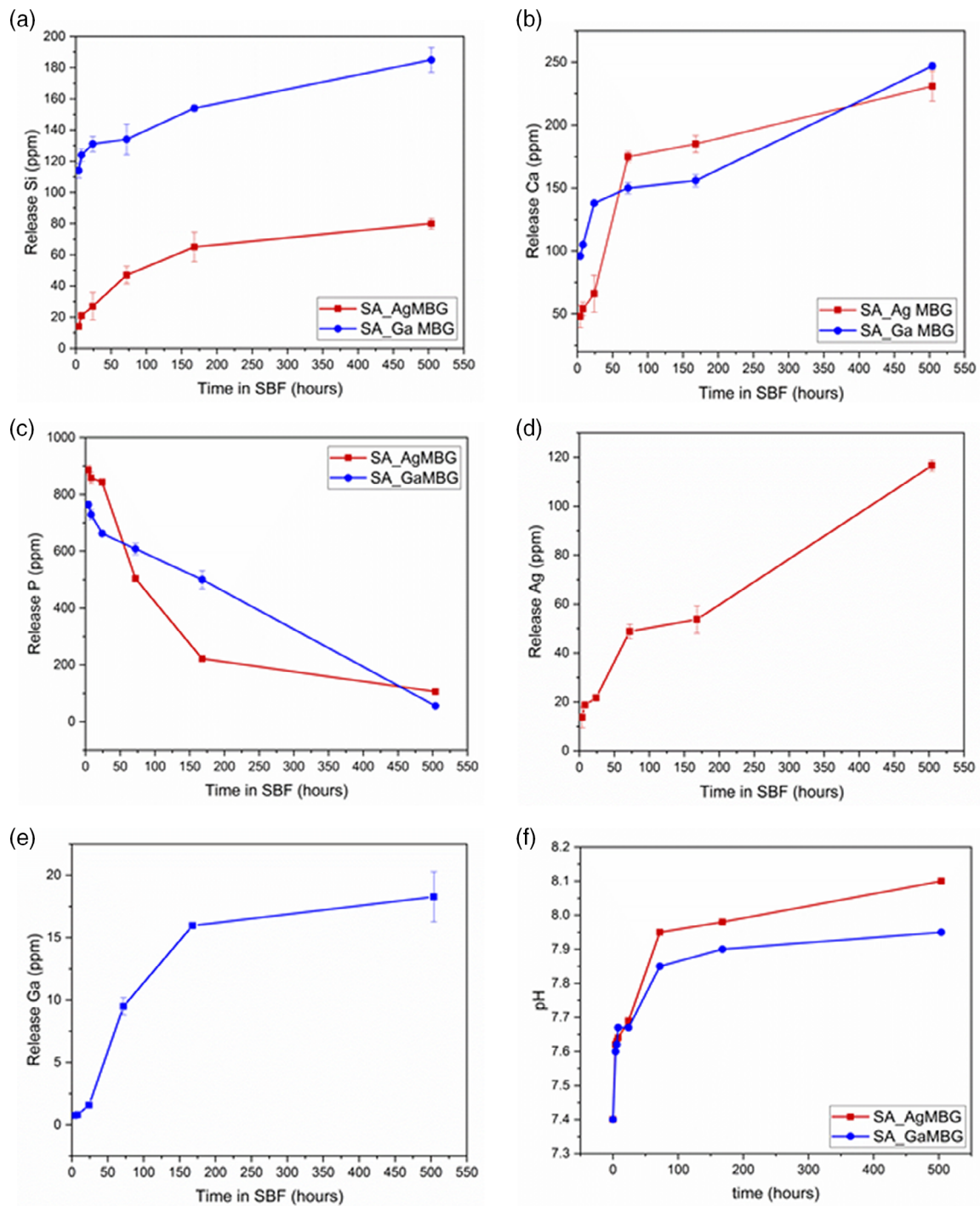


**FIGURE 12** Profiles of the release of ions as a function of time in SBF for SA\_Ag-MBG and SA\_Ga-MBG BG scaffolds. The pH variation is also shown

SEM observation confirmed the presence of the MBG coatings and SBF immersion tests for up to 7 days showed the ability of the scaffolds to form HCA on their surfaces. As a consequence of immersion in SBF, the porosity of the scaffolds increased over time, reaching a value of 90% after 28 days of immersion. These results are in good agreement with those found in previous studies.<sup>40</sup> Scaffolds were also tested in terms of mechanical properties before and after immersion

in SBF. The as-fabricated samples showed a maximum compressive strength of  $4 \pm 1$  MPa, a value in the range of those found for spongy bone (2–12 MPa). The achievement of improved mechanical properties, as already discussed in previous studies,<sup>41</sup> is the result of the lower porosity of the natural marine sponges in comparison to the polyurethane sponges traditionally used to make this type of scaffolds.<sup>16</sup> Natural marine sponges are also characterized by pores in the



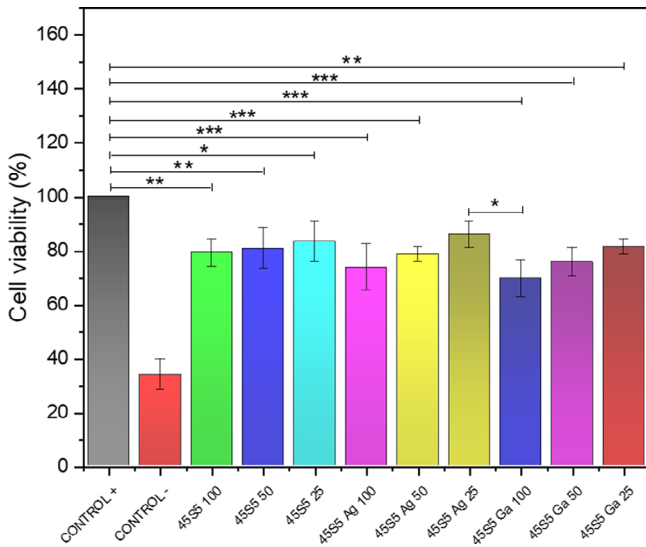


**FIGURE 13** Relative viability of MC3T3-E1 cells cultured with ionic dissolution products of SA\_Ag-MBG and SA\_Ga-MBG BG scaffolds. Significance levels: \* $p < .05$ , \*\* $p < .01$ , \*\*\* $p < .001$  (Bonferroni's post-hoc test was used)

range  $<200 \mu\text{m}$ , which are important for adhesion, migration, and proliferation of cells on the scaffold.<sup>42</sup> These pores in fact allow biological fluids to reach the inner core of the porous scaffold, and thus integration with the surrounding tissue is facilitated.<sup>43</sup> Macropores in the  $200\text{--}500 \mu\text{m}$  range, beneficial for osteointegration and neovascularization,<sup>44,45</sup> were also part of the structure of the scaffolds. Mechanical properties decreased after 1 week of immersion in SBF (reaching a value of  $1.0 \pm 0.6 \text{ MPa}$ ) due to the degradation of the BG scaffolds in contact with water-based solutions.

The ion release capability of the coated BG-based scaffolds was also tested. From the ion release profiles, it was possible to observe that the release of Si, Ca, and P ions takes place immediately for both scaffold types. The decrease of P concentration over time suggested the formation of a P-containing layer on the surface of the scaffolds during soaking in SBF. The therapeutic ions (Ag and Ga) were also detected. The release profile of Ag did not increase linearly potentially due to the deposit of insoluble AgCl, while the Ga ion release profile increased continuously, showing a controlled and sustained release. Agar diffusion tests were performed against Gram-positive and Gram-negative bacteria and showed promising results against both strains. A

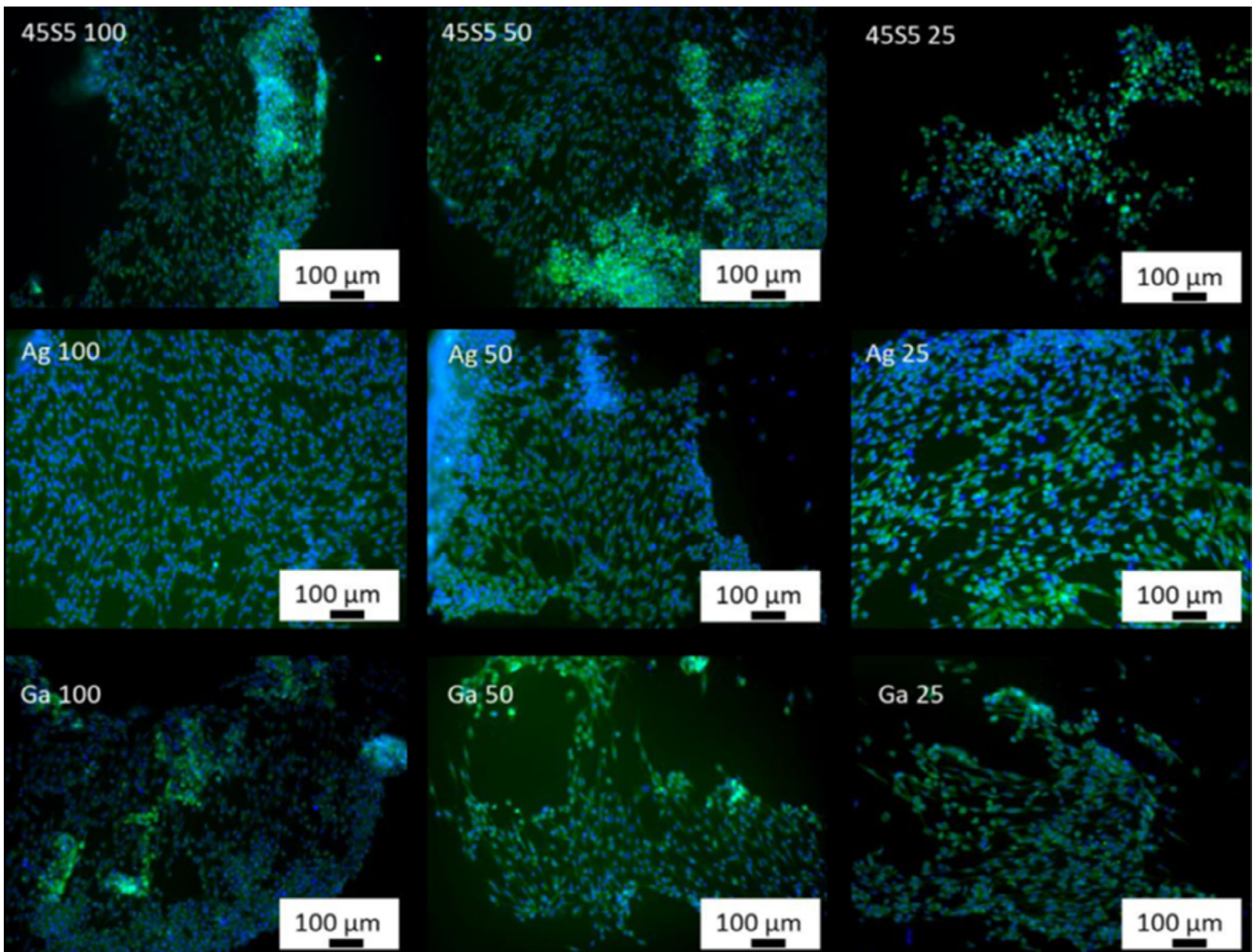


**FIGURE 14** Fluorescence microscopy images of calcein/DAPI stained MC3T3-E1 cells cultured with different concentrations (100, 50, and 25%) of ionic dissolution products of coated and uncoated BG-based scaffolds



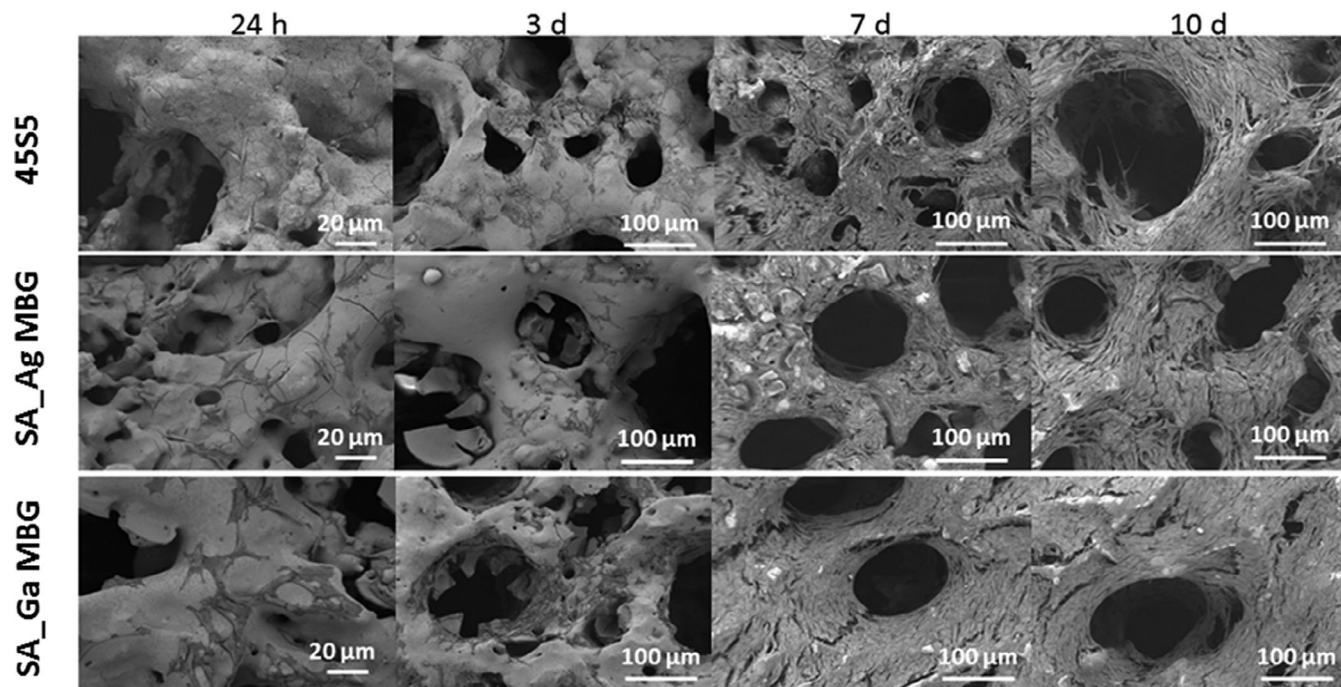


**FIGURE 15** SEM micrographs showing cell adhesion on the surface of 45S5, Ag-, and Ga-MBG coated BG scaffolds after 1, 3, 7 and 10 days of incubation

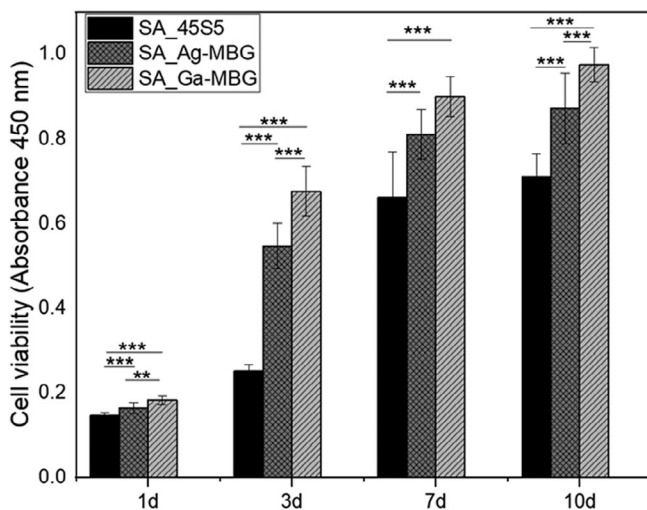


**FIGURE 16** Viability of MC3T3-E1 cells cultured directly in contact with uncoated and coated scaffolds for 1, 3, 7, and 10 days. Significance levels: \* $p < .05$ , \*\* $p < .01$ , \*\*\* $p < .001$  (Bonferroni's post-hoc test was used)

significant inhibition zone was observed for both bacterial strains after 24 hr of incubation. Tests were also carried out for samples up to 3 days after immersion in SBF to ensure their antibacterial properties. Even after 3 days of soaking in SBF the antibacterial properties of the coated scaffolds were retained. Furthermore, cytocompatibility tests were performed. Indirect and direct cell culture tests were carried out according to the general guidance of the International Standardization Organization (ISO 10993-5-2009). The extracted media from Ag- and

Ga-MBG coated scaffolds did not show toxicity or negative effects on cell viability. Direct cell culture tests were performed after the scaffold had been subjected to a pre-conditioning treatment, which was carried out to avoid a rapid increase of pH during cell culture experiments.<sup>35</sup> To better mimic the physiological condition, the medium was changed every day. Previous studies have shown that refreshing the medium every 2–3 days leads to a “more biocompatible” surface for cell culture studies.<sup>44,46,47</sup> Considering the possibility that during the pre-conditioning treatment therapeutic ions can be leaked from the present system, EDS analysis was performed on pre-treated samples. EDS indicated that the therapeutic ions were still present in the coating. In addition, the differences in cell viability found between the BG compositions with different ion doping were considered an indirect evidence of the presence of the ions. As the ions are the only major difference between samples, variations in cell culture outputs are most probably caused by the effect that the ions have on MC3T3-E1 cells. Cell viability was found to be low after 24 hr of culture. These results can have two possible explanations: (a) after 24 hr cells did not have enough time to grow; (b) it might be possible that part of the cells seeded into the scaffold flowed out of the sample and were lost, when the scaffolds were transferred on a new plate for the WST-8 assay. However, after 3 days of incubation, cells started to proliferate and after 7 days they completely colonized the scaffolds. The production of VEGF was also quantitatively measured. The expression of VEGF was found to be higher when cells were placed in contact with Ga-MBG-coated scaffolds compared to uncoated 45S5 BG scaffolds. Results of VEGF measurement were in agreement with those found for the WST-8 assay. Moreover, LDH was measured after 7 and 10 days of incubation. No significant differences were observed

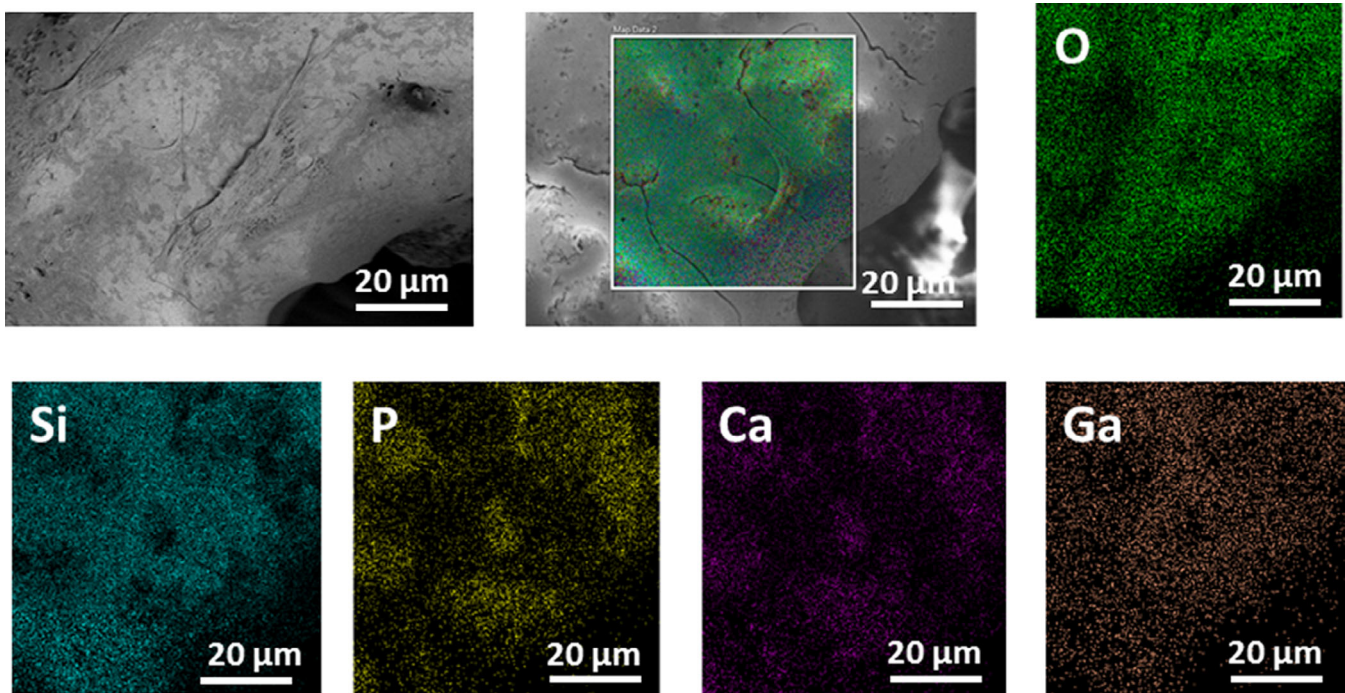


**FIGURE 17** EDS analysis showing the presence of the biologically active ion (Ga) after pre-conditioning treatment used for the direct cell culture tests

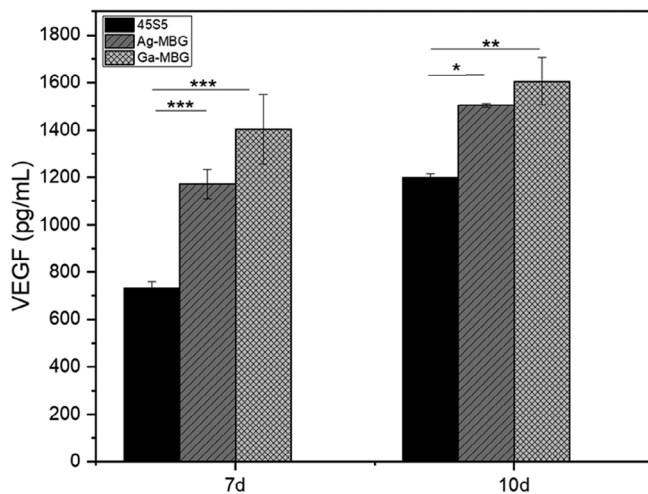


**FIGURE 18** VEGF release from MC3T3-E1 cells treated with uncoated 45S5-based scaffolds and Ag- and Ga-MBG coated scaffolds. Asterisks denote significant differences compared with the reference, \*\*\* $p < .001$  (Bonferroni's post hoc test was used)

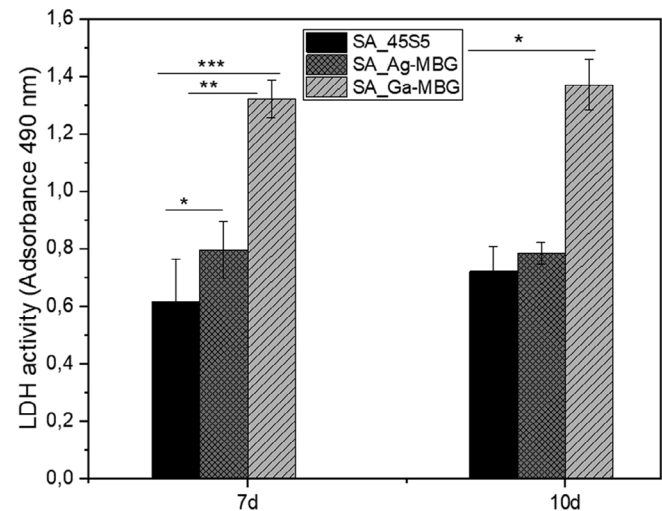


**FIGURE 19** LDH activity of MC3T3-E1 cells (absorbance 490–690 nm) on different samples after 7 and 10 days of incubation. Significance levels: \* $p < .05$ , \*\* $p < .01$ , \*\*\* $p < .001$  (Bonferroni's post hoc test was used)

between the two incubation times, suggesting that cells after 7 days stopped proliferating and started to differentiate. This hypothesis was confirmed by quantitatively measuring osteocalcin production. The coated scaffolds seemed to support the late stage of osteoblast differentiation.

The differentiation of pre-osteoblast cells on Ga-MBGs has also been studied by Gomez-Cerezo et al<sup>48</sup>, who measured the ALP

activity after 7 days in presence of 1 mg/ml MBGs. The authors obtained similar results to those found in this work. A higher ALP phosphatase activity was expressed by MC3T3-E1 cells in presence of MBGs containing gallium in comparison to the Ga-free analogues.<sup>48</sup> The higher ALP activity of pre-osteoblasts in contact with Ga-MBGs indicates that Ga ions provide biological signals to stimulate cell differentiation toward bone forming cells.<sup>48</sup> Bernstein<sup>49</sup> and



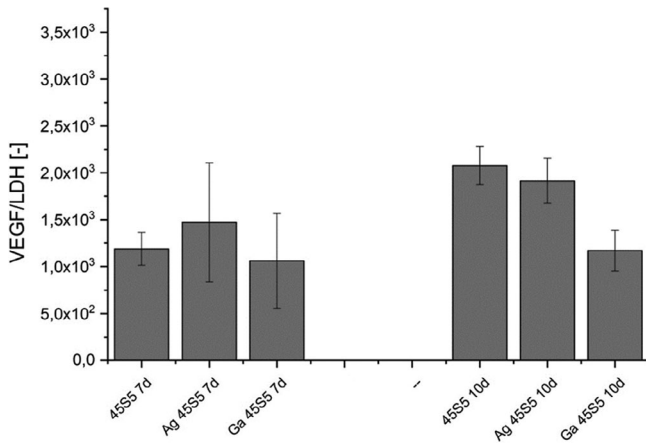


**FIGURE 20** VEGF/LDH expression of uncoated 45S5 BG scaffolds, and Ag- and Ga-MBG-coated scaffolds after 7 and 10 days of incubation

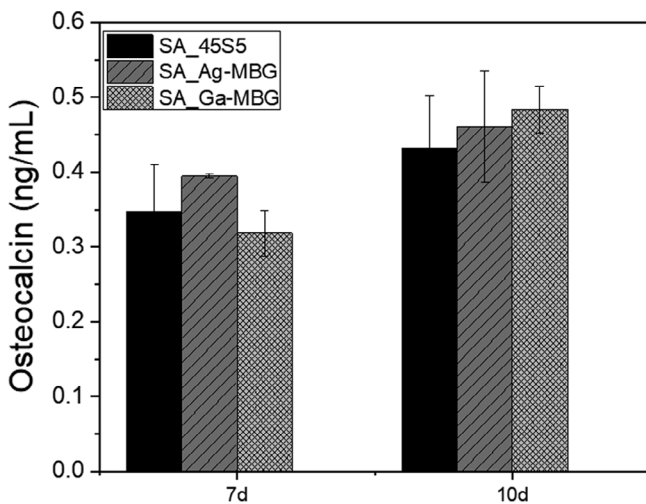
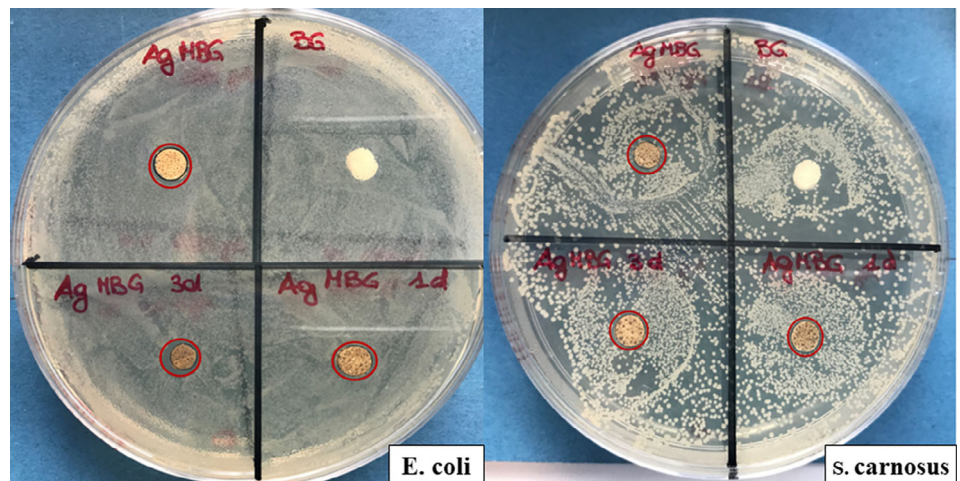


**FIGURE 21** Osteocalcin production of uncoated and coated scaffolds after 7 and 10 days of incubation. Significance levels: \* $p < .05$ , \*\* $p < .01$ , \*\*\* $p < .001$  (Bonferroni's post-hoc test was used)

**FIGURE 22** Results of antibacterial tests showing the effect of SA\_Ag-MBG scaffolds before and after immersion in SBF after 24 hr of incubation against Gram-positive (*S. carnosus*) and Gram-negative (*E. coli*) bacteria



Bockman et al<sup>50</sup> found that the level of plasma alkaline phosphatase, a marker for bone formation, and the bone calcium content in gallium nitrate-treated rats can increase in the presence of gallium. On the contrary, the incorporation of Ag<sup>+</sup> in mesoporous bioactive glasses seems to have little influence on cell differentiation. Similar results were obtained by Zhu et al,<sup>51</sup> who investigate the biological behavior of silver containing mesoporous 58S bioactive glass. The results obtained in this work showed that ion-doped MBGs-coated scaffolds have potential for applications in bone tissue engineering with specific ions, in the present case Ag and Ga, having different biological effects.

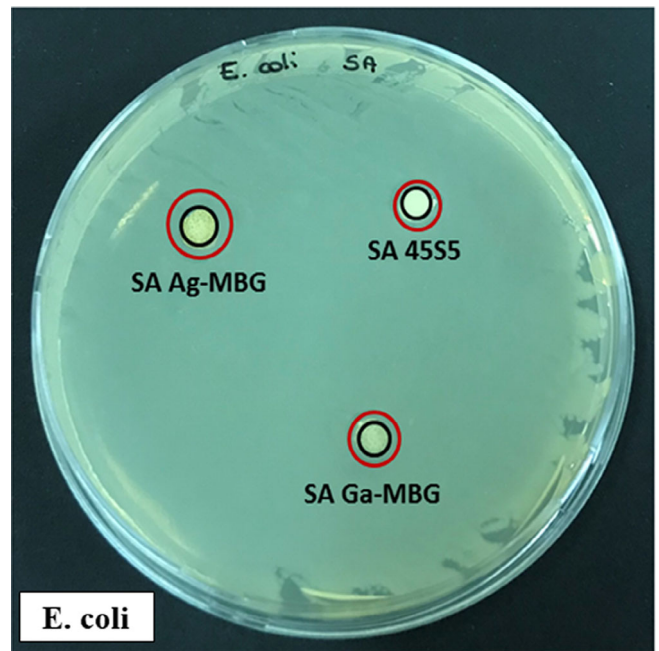


**FIGURE 23** Results of antibacterial test showing the effect of SA\_Ag-MBG and SA\_Ga-MBG-scaffolds against Gram negative (*E. coli*) bacteria compared to non-coated 45S5 BG scaffold (SA 45S5)

## 5 | CONCLUSIONS

Natural marine sponges were selected as sacrificial templates for the fabrication of bioactive-based scaffolds for bone tissue engineering. BG scaffolds were produced by the foam replica technique and successfully coated with a silicate sol solution to form Ag- or Ga-doped MBG coatings. The samples were characterized by relatively high mechanical properties (~4 MPa), high bioactivity and antibacterial properties. Moreover, the coated scaffolds showed good biocompatibility verified by MC3T3-E1 pre-osteoblastic cells thus representing a new family of antibacterial scaffolds for bone tissue engineering.

### ACKNOWLEDGMENTS

This research was carried out within the EU Horizon 2020 framework project COACH (ITN-ETN, Grant agreement nr. 642557). W. H. Goldmann thanks the German Science Foundation (DFG, Go598) for financial support. The authors thank Astrid Mainka (FAU) for technical advice. The authors would like to thank the TEM facilities of CITIUS-US. TEM analysis was funded by the Grant P2017/837-University of Seville (Spain). The authors thank Prof. Enrica Vernè and Dr Marta Miola (Politecnico di Torino, Italy) for the technical support and the help with the ICP analyses.

Open access funding enabled and organized by Projekt DEAL.

### ORCID

Ana M. Beltrán  <https://orcid.org/0000-0003-2599-5908>

Aldo R. Boccaccini  <https://orcid.org/0000-0002-7377-2955>

### REFERENCES

- Gómez-Barrena E, Rosset P, Lozano D, Stanovici J, Ernthaller C, Gerhard F. Bone fracture healing: cell therapy in delayed unions and nonunions. *Bone*. 2015;70:93-101.
- Amini AR, Laurencin CT, Nukavarapu SP. Bone tissue engineering: recent advances and challenges. *Crit Rev Biomed Eng*. 2012;40:363-408.
- Arrington ED, Smith WJ, Chambers HG, Bucknell AL, Davino NA. Complications of iliac crest bone graft harvesting. *Clin Orthop Relat Res*. 1996;329:300-309.
- Eisenbarth E. Biomaterials for tissue engineering. *Adv Eng Mater*. 2007;9:1051-1060.
- Porter JR, Ruckh TT, Popat KC. Bone tissue engineering: a review in bone biomimetics and drug delivery strategies. *Biotechnol Prog*. 2009;25(6):1539-1560.
- Boccardi E, Philippart A, Juhasz-Bortuzzo JA, Novajra G, Vitale-Brovarone C, Boccaccini AR. Characterisation of bioglass based foams developed via replication of natural marine sponges. *Adv Appl Ceram*. 2015;6753:S56-S62.
- Hench LL, Splinter RJ, Allen WC, Greenlee TK. Bonding mechanisms at the interface of ceramic prosthetic materials. *J Biomed Mater Res*. 1971;5:117-141.
- Hench LL. Bioceramics: from concept to clinic. *J Am Ceram Soc*. 1991;74:1487.
- Hench LL. The story of bioglass. *J Mater Sci Mater Med*. 2006;17:967-978.
- Gerhardt L-C, Boccaccini AR. Bioactive glass and glass-ceramic scaffolds for bone tissue engineering. *Materials (Basel)*. 2010;3:3867-3910.
- Jones JR. Review of bioactive glass: from Hench to hybrids. *Acta Biomater*. 2013;9:4457-4486.
- Hoppe A, Güldal NS, Boccaccini AR. A review of the biological response to ionic dissolution products from bioactive glasses and glass-ceramics. *Biomaterials*. 2011;32:2757-2774.
- Gorustovich AA, Roether JA, Boccaccini AR. Effect of bioactive glasses on angiogenesis: a review of in vitro and in vivo evidences. *Tissue Eng Part B Rev*. 2010;16:199-207.
- Xynos ID, Hukkanen MVJJ, Batten JJ, Buttery LD, Hench LL, Polak JM. Bioglass 45S5 stimulates osteoblast turnover and enhances bone formation in vitro: implications and applications for bone tissue engineering. *Calcif Tissue Int*. 2000;67:321-329.
- Boccardi E, Ciraldo FE, Boccaccini AR. Bioactive glass-ceramic scaffolds: processing and properties. *MRS Bull*. 2017;42:226-232.
- Chen QZ, Thompson ID, Boccaccini AR. 45S5 bioglass-derived glass-ceramic scaffolds for bone tissue engineering. *Biomaterials*. 2006;27:2414.
- Boccardi E, Melli V, Catignoli G, et al. Study of the mechanical stability and bioactivity of bioglass® based glass-ceramic scaffolds produced via powder metallurgy-inspired technology. *Biomed Mater*. 2016;11:015005.
- Aguilar-Reyes EA, León-Patiño CA, Jacinto-Diaz B, Lefebvre L-P. Structural characterization and mechanical evaluation of bioactive glass 45S5 foams obtained by a powder technology approach. *J Am Ceram Soc*. 2012;95:3776-3780.
- Boccardi E, Belova IV, Murch GE, Boccaccini AR, Fiedler T. Oxygen diffusion in marine-derived tissue engineering scaffolds. *J Mater Sci Mater Med*. 2015;26:200.
- Manzano M, Colilla M, Vallet-Regí M. Drug delivery from ordered mesoporous matrices. *Expert Opin Drug Deliv*. 2009;6:1383-1400.
- Manzano M, Vallet-Regí M. New developments in ordered mesoporous materials for drug delivery. *J Mater Chem*. 2010;20:5593.
- Vallet-Regí MC, García MM, & Colilla, M. Mesoporous ceramics as drug delivery systems. *Biomedical applications of mesoporous ceramics: Drug delivery, smart materials and bone tissue engineering*. Boca Raton - London - New York: CRC Press; 2013:67-104.
- Kargozar S, Montazerian M, Hamzehlou S, Kim H-W, Baino F. Mesoporous bioactive glasses: promising platforms for antibacterial strategies. *Acta Biomater*. 2018;81(1-19):1-19.
- Drago L, Toscano M, Bottagisio M. Recent evidence on bioactive glass antimicrobial and Antibiofilm activity: a mini-review. *Materials*. 2018;11:326.
- Vallet-Regí M, Salinas AJ. Mesoporous bioactive glasses in tissue engineering and drug delivery. In: Boccaccini AR, Brauer DS, Hupa L, eds. *Bioactive Glasses: Fundamentals, Technology and Applications*. London, England: The Royal Society of Chemistry; 2017:393-419.
- Zhao D, Wan Y, Zhou W. *Ordered Mesoporous Materials*. Weinheim, Germany: Wiley-VCH Verlag GmbH & co. KGaA; 2013.
- Wu C, Chang J. Mesoporous bioactive glasses: structure characteristics, drug/growth factor delivery and bone regeneration application. *Interface Focus*. 2012;2:292-306.
- Kaya S, Cresswell M, Boccaccini AR. Mesoporous silica-based bioactive glasses for antibiotic-free antibacterial applications. *Mater Sci Eng C*. 2018;83:99-107.
- Philippart A, Gómez-Cerezo N, Arcos D, et al. Novel ion-doped mesoporous glasses for bone tissue engineering: study of their structural characteristics influenced by the presence of phosphorous oxide. *J Non Cryst Solids*. 2017;455:90-97.
- Wu C, Chang J. Multifunctional mesoporous bioactive glasses for effective delivery of therapeutic ions and drug/growth factors. *J Control Release*. 2014;193:282-295.
- Kokubo T, Takadama H. How useful is SBF in predicting in vivo bone bioactivity? *Biomaterials*. 2006;27:2907-2915.
- Ciraldo F, Liverani L, Gritsch L, Goldmann WH, Boccaccini AR. Synthesis and characterization of silver-doped Mesoporous bioactive

- glass and its applications in conjunction with electrospinning. *Materials (Basel)*. 2018;11:692.
33. Lopez-Noriega A, Arcos D, Izquierdo-Barba I, Sakamoto Y, Terasaki O, Vallet-Regí M. Ordered mesoporous bioactive glasses for bone tissue regeneration. *Chem Mater*. 2006;18:3137.
  34. Zheng K, Solodovnyk A, Li W, et al. Aging time and temperature effects on the structure and bioactivity of gel-derived 45S5 glass-ceramics. *J Am Ceram Soc*. 2015;98:30-38.
  35. Ciraldo FE, Boccardi E, Melli V, Westhauser F, Boccacchini AR. Tackling bioactive glass excessive in vitro bioreactivity: preconditioning approaches for cell culture tests. *Acta Biomater*. 2018;75:3-10.
  36. Sanchez-Salcedo S, Malavasi G, Salinas AJ, et al. Highly-bioreactive silica-based Mesoporous bioactive glasses enriched with gallium(III). *Materials (Basel, Switzerland)*. 2018;11:367
  37. Arnett TR. Extracellular pH regulates bone cell function. *J Nutr*. 2008; 415:415S-418S.
  38. Christenson RH. Biochemical markers of bone metabolism: an overview. *Clin Biochem*. 1997;30:573-593.
  39. Zhang Y, Zhang M. Cell growth and function on calcium phosphate reinforced chitosan scaffolds. *J Mater Sci Mater Med*. 2004;15:255-260.
  40. Boccardi E, Natural Marine Derived Bioactive Glass Based Scaffolds with Improved Functionalities, Dissertation, University of Erlangen-Nuremberg, 2016, [urn:nbn:de:bvb:29-opus4-82329](https://nbn-resolving.org/urn:nbn:de:bvb:29-opus4-82329).
  41. Boccardi E, Philippart A, Melli V, et al. Bioactivity and mechanical stability of 45S5 bioactive glass scaffolds based on natural marine sponges. *Ann Biomed Eng*. 2016;1881-1893.
  42. Cunningham E, Dunne N, Walker G, Maggs C, Wilcox R, Buchanan F. Hydroxyapatite bone substitutes developed via replication of natural marine sponges. *J Mater Sci Mater Med*. 2010;21:2255-2261.
  43. Crovace MC, Souza MT, Chinaglia CR, Peitl O, Zanotto ED. Biosilicate® – a multipurpose, highly bioactive glass-ceramic. In vitro, in vivo and clinical trials. *J Non Cryst Solids*. 2016;432:90-110.
  44. El-Ghannam A, Ducheyne P, Shapiro IM. Bioactive material template for in vitro synthesis of bone. *J Biomed Mater Res*. 1995;29(3):359-370.
  45. El-Ghannam A, Ducheyne P, Shapiro IM. Formation of surface reaction products on bioactive glass and their effects on the expression of the osteoblastic phenotype and the deposition of mineralized extracellular matrix. *Biomaterials*. 1997;18:295-303.
  46. Vitale-Brovarone C, Verné E, Robiglio L, et al. Development of glass-ceramic scaffolds for bone tissue engineering: characterisation, proliferation of human osteoblasts and nodule formation. *Acta Biomater*. 2007;3:199-208.
  47. Verne E, Bretcanu O, Balagna C, et al. Early stage reactivity and in vitro behavior of silica-based bioactive glasses and glass-ceramics. *J Mater Sci Mater Med*. 2009;75:75-87.
  48. Gómez-Cerezo N, Verron E, Montouillout V, et al. The response of pre-osteoblasts and osteoclasts to gallium containing mesoporous bioactive glasses. *Acta Biomater*. 2018;76:333-343.
  49. Bernstein LR. Mechanisms of therapeutic activity for gallium. *Pharmacol Rev*. 1998;50:665.
  50. Bockman R. The effects of gallium nitrate on bone resorption. *Semin Oncol*. 2003;30(5):12.
  51. Zhu H, Hu C, Zhang F, et al. Preparation and antibacterial property of silver-containing mesoporous 58S bioactive glass. *Mater Sci Eng C*. 2014;42:22-30.

**How to cite this article:** Ciraldo FE, Arango-Ospina M, Goldmann WH, et al. Fabrication and characterization of Ag- and Ga-doped mesoporous glass-coated scaffolds based on natural marine sponges with improved mechanical properties. *J Biomed Mater Res*. 2021;109:1309–1327. <https://doi.org/10.1002/jbm.a.37123>